IMPROVEMENTS IN SIMULATING DISCRETE DEPOSITION MODELS

A THESIS SUBMITTED TO
THE GRADUATE SCHOOL OF ENGINEERING AND SCIENCE
OF BILKENT UNIVERSITY
IN PARTIAL FULFILLMENT OF THE REQUIREMENTS FOR
THE DEGREE OF
MASTER OF SCIENCE
IN
PHYSICS

By
Batoul Hashemi
November 2021

Improvements In Simulating Discrete Deposition Models

By Batoul Hashemi

November 2021

We certify that we have read this thesis and that in our opinion it is fully adequate, in scope and in quality, as a thesis for the degree of Master of Science.

Fatih Ömer Ilday(Advisor)

Hande Toffoli

Bilal Tanatar

Approved for the Graduate School of Engineering and Science:

Ezhan Karaşan
Director of the Graduate School

ABSTRACT

IMPROVEMENTS IN SIMULATING DISCRETE DEPOSITION MODELS

Batoul Hashemi
M.S. in Physics
Advisor: Fatih Ömer Ilday
November 2021

The main purpose of this work is to describe the surface growth phenomena. Initially, we give a brief introduction to the analytical studies, in particular, done by differential equations such as Edward-Wilkinson and Kardar-Parisi-Zhang equations, and then introduce the discrete surface growth models as a means to describe these phenomena with a restricted number of rules. The universality properties of these models help us categorize them in three different classes, namely Gaussian, Edward-Wilkinson, and Kardar-Parisi-Zhang universality classes. Five different numerical growth models are explained, and the statistical properties of the growing interfaces in 1D systems are examined via computational studies. Growth properties of 1D structures are viewed in two different ways, one being the scaling exponent of roughness changing with respect to time, and the other the distribution of height fluctuations. In this research, we show that our numerical simulation findings are in accord with the theoretical and analytical predictions. In addition, for the ballistic deposition and restricted solid-on-solid models, we introduce a binning method [1] which improves our numerical results. Moreover, we propose a novel modification on the ballistic deposition model by detecting the thin-deep wells on the interface and average them out which enables us to report an improvement in our numerical results with a noteworthy development on physical properties of the system. Furthermore, we investigate the effect of the change of the deposition rate on the universal behavior of the system, as a result, we introduce critical values for the deposition rate with respect to the size of the system. With these modifications, we are one step closer to defining the complex behavior of the growth phenomena.

Keywords: Surface growth, KPZ equation, Ballistic deposition, Random deposition, Random deposition with surface diffusion, Eden model, Restricted solid-on-solid model, Tracy-Widom distribution.

ÖZET

AYRIK BİRİKTİRME MODELLERİNİN SİMÜLASYONUNDA GELİŞMELER

Batoul Hashemi
Fizik, Yüksek Lisans
Tez Danışmanı: Doç. Dr. Fatih Ömer İlday
Kasim 2021

Bu çalışmanın temel amacı, yüzey büyüme olaylarını tanımlamaktır. İlk olarak, Edward-Wilkinson ve Kardar-Parisi-Zhang denklemleri gibi diferansiyel denklemlerle yapılan analitik çalışmalara kısa bir giriş yapıldıktan sonra bu sistemleri sınırlı kurallarla ifade eden ayrık yüzey büyüme modellerinden bahsedilmiştir. Bu modellerin evrensel kısımlarının özellikleri en çok bilinen üç farklı sınıfla tanımlanabilir: Gaussian, Edward-Wilkinson ve Kardar-Parisi-Zhang . Bes farklı sayısal buyume modeli incelenmiş ve 1B sistemlerde büyüyen arayüzlerin istatistiksel özellikleri bilgisayar simülasyonları kullanılarak hesaplanmiştir. 1B yapıların büyüme özellikleri, birim zamana göre değişkenlik gösteren pürüzlülüğün ölçeklendirme üssü ve yükseklik dalgalanmalarının dağılımı olmak üzere iki farklı şekilde incelenmiştir. Beş farklı sayısal büyüme modeli açıklanmış ve istatistiksel özellikleri hesaplama ile incelenmiştir. 1B yapıların büyüme özellikleri, biri zamana göre değişen pürüzlülüğün ölçeklendirme üssü ve diğeri yükseklik dalgalanmalarının dağılımı olmak üzere iki farklı şekilde incelenir. Bu araştırmada, sayısal simülasyon bulgularımızın teorik ve analitik tahminlerle uyumlu olduğunu gösteriyoruz. Ek olarak, balistik biriktirme ve kısıtlı katı-katı modelleri için, sayısal sonuçlarımızı iyileştiren bir gruplama yöntemi [1] sunuyoruz. Ayrıca, balistik biriktirme modelinde, ara yüzeydeki ince-derin kuyuları tespit ederek ve ortalamalarını alarak, sistemin fiziksel özelliklerinde kayda değer bir gelişme ile sayısal sonuçlarımızda bir iyileşme rapor etmemizi sağlayan yeni bir modifikasyon öneriyoruz. Ayrıca, birikme hızı değişiminin sistemin evrensel davranışı üzerindeki etkisini araştırdık, sonuç olarak, sistemin boyutuna göre biriktirme hızı için kritik değerler ortaya koyduk.

Anahtar sözcükler: Yüzey büyüme, KPZ denklemi, Ballistic modellemesi, Rastgele model, Eden model, RSOS model, Tracy-Widom dağılımı.

Acknowledgement

I want to thank Dr. Ömer Ilday for his supervision and support. I also want to thank Dr. Serim Ilday for her inspiring work and guidance. I should thank Dr. Ghaith Makey for his guidance and providing the initial code for the deposition models. Many thanks to Dr. Tanatar and Dr. Toffoli for their instructive revisions and feedback.

I want to thank Selçuk Parlak and my coworker Xhulian Lickollari for their support and companionship which cannot be underestimated. There are so many people I want to thank but I should mention Aysu Başak Altuğ, Yetkin Pulcu, and Oğuzhan Oğuz for their friendship and support during the pandemic and thesis. I want to express my deep gratitude to my family for always be there for me and supporting me throughout my life. I can't thank my family enough for all that they have done for me.

Dedicated to my family; my mom Azam, my brother Amin and my father Hamidreza...

Contents

List of Figures

List of Tables

Chapter 1

Introduction

There has been historical interest in growth phenomena, initially motivated by the desire to explain the shape of plants or animals. A well-known treatise on this subject is by D'Arcy W. Thompson and titled "On Growth and Form." In recent decades, interest in growth has broadened to encompass not only the question of "why things in nature are of certain shapes," to the cause and the dynamics of the growth process. The relevant questions started to include the microscopic perspective as means to explain how growth happens.

Although the motivation for understanding the growth phenomena was originally to explain biological growth, by now there is a vast literature exploring various types of growth using physical and mathematical concepts. Additionally, interest in the growth process is not limited to biological structures, and there is much interest in growth in various physical systems, particularly at the microscopic and nanoscale as that occurs during, for example, vacuum deposition systems. A curious aspect is that growth observed in entirely different physical systems have been found to have similar statistical properties that fall into several distinct cases. Within each case, one observes a certain level of universality, meaning that the broad features of the growth turn out to be independent of the many details of the systems that fall within that group.

At first glance, defining the growth process may seem trivial, but the physical and mathematical definition of the growth phenomena is a challenging topic in non-equilibrium statistical physics. For gaining a better perspective on the growth phenomena, we study the statistical properties of the interfaces. We also present an improvement of the models.

In chapter 2, the theoretical properties of universality classes are discussed. We discuss three universality classes, namely the Gaussian, Edward-Wilkinson, and Kardar-Parisi-Zhang classes. These classes show universal behavior due to their invariancy under certain symmetries and scaling exponents. For the discrete growth models, we discuss that the height fluctuations of the interfaces follow specific distributions. The probability density function (PDF) of height fluctuations converges to the Gaussian distribution for the pure random deposition and random deposition with surface diffusion models. For the Eden, ballistic, and restricted solid-on-solid models, the PDF follows the Tracy Widom distribution.

In chapter 3, we numerically investigate the statistical properties of some discrete models, including random deposition, random deposition with surface diffusion, ballistic deposition, Eden, and restricted solid-on-solid models. We investigate the universality class to which each model fits by calculating the surface roughness exponents and height fluctuations distribution.

In chapter 4, we introduce new methods for the simulation of the interface and the statistical properties of the Ballistic deposition model. These methods use the well-known binning method and a new method introduced in this thesis, which we refer to as the restriction factor method.

In the final chapter of the thesis, we examine the effect of the deposition rate on the ballistic and restricted solid on solid deposition models with a combination of methods that are introduced in chapter 4.

We conclude the thesis by discussing the best results for the statistical properties of the models and suggestions of future work for further improvements for models to have a better fit to real-life experiments.

Chapter 2

Universal Behavior of Growth Models

The surface growth phenomena are ubiquitous. We confront surfaces everywhere. Those surfaces can be static or dynamic. The dynamic ones are readily observed to grow or shrink, but even the seemingly static ones may be engaged in a slow process of transformation, such as the surface of rocks. Surfaces can be shrunk by processes like erosion or etching, and they can grow by processes like deposition, which can happen from the "outside" as in snow falling, or from the "inside" as in paper wetting if the flow of water is thought as a deposition of water toward the interface.

One main characteristic of the surface is its roughness, but it is scale-dependent along with most of the other properties. A surface may appear very smooth on a large scale, such as when observed visually from a distance. The same surface looks increasingly rough, on a smaller scale, such as when observed under a microscope.

When we study the roughness of these surfaces and how the roughness changes as the interface evolves through the growth process, we see that many different surfaces with different scales and compositions seem to be very similar. This similarity is what lets us classify them into very big universality classes. Surfaces as small in scale as the surface of human cells up to surfaces as big as the surface of planets can have more in common than we think.

Here, we will deal with surfaces growing by the process of deposition from the "outside," just as the surface of a sandpile is increased when grains of sand are continuously being thrown at it. We are particularly interested in the universal behaviors of such surfaces. We are motivated that identifying such features holds valuable clues to a more complete understanding of the processes involved and, much more importantly, may lead to a general theoretical framework of far-from-thermal equilibrium systems. On a more practical note, universality may help translate understanding of, say, self-assembly- or deposition-based growth to seemingly unrelated problems such as the growth of bacterial colonies or the large forest areas.

We can think of a straightforward form of surface growth (known as the 1+1 dimensional case) as having a random deposition of particles (e.g., grains of sand) over initially a smooth line of particles as the ground of the system. As those particles are deposited, the initially smooth interface is moving upward and becoming rougher. The height of the interface is increasing on average, but we also see that the height over some portions of the line-ground is increasing more than in other portions. This behavior is responsible for the roughness of the interface, which is usually interpreted as the array of spatial fluctuations of the interface.

2.1 Universality Classes

2.1.1 Gaussian Universality Class

The most straightforward way to describe the surface growth phenomena is to define a force term which controls the fluctuations of the interface in the following way,

$$\frac{\partial h(x,t)}{\partial t} = \eta(x,t), \tag{2.1}$$

where here $h(x,t)$ stands for height depending on both position and time, and $\eta(x,t)$ is uncorrelated noise considered to be random Gaussian white noise with

$$< \eta(x,t) >= 0, \tag{2.2}$$

Gaussian white noise has the zero mean of as it is mentioned in equation 2.2, hence there is no correlation in the noise term.

$$< \eta(x',t')\eta(x,t) >= 2D\delta(x-x')\delta(t-t'). \tag{2.3}$$

With this equation, we are able to describe the roughness of the interface and its change with time. If we add a constant velocity term to describe the average growth (moving upward of the interface), we get the most straightforward equation describing the growth phenomena. However, in this model, all points along the surface grow completely independently. Any lateral growth or diffusion across the surface is missing. The presence of diffusion contributes to a smoother interface.

In growing interfaces, there are certain properties such as surface width or roughness, particle velocity, free energy, particle current, and height fluctuations. Here we are investigating the width of the surface, which is related to the 'amplitude' of the height fluctuations, and the probability distribution of these fluctuations.

From the above equation, if we look for the surface width, we will see that it increases in time as: $w(t) = \sqrt{< h^2 > - < h >^2} = \sqrt{2Dt}$ This is the dependence of the width over time for the simplest type of growth. We described it with the simple analytic equation above, but this type of growth also corresponds to the simplest kind of discrete deposition model, which is the random deposition. Since the growth exponent of the width is always 1/2, thus independent of any parameter in the equation, it becomes a universal characteristic feature of this class. The other main characteristic is that the probability distribution of the height fluctuations is always a Gaussian distribution, from where the name of the class is coming.

The earliest example of Gaussian universality was discovered through a simple thought experiment. The main question was, if a coin flipped N times, what would be the outcome of this experiment? The outcome of a single flip has a chance to be heads or tails with probabilities 1/2 for each outcome. If these independent experiments are repeated N times, we have a probability of $1/2^N$, and we expect to encounter heads N/2 times. Of course, this does not have a direct correspondence to the real outcome. The outcome of the experiment can vary from the original expectation with a scale of $\sqrt{N}$. In continuous terms, the probability distribution of heads was found to correspond to the Gaussian distribution. After further examination of the experiment, it was realized that this behavior could be generalized to any independent and identically distributed random variables. In mathematical terms, the cumulative distribution function (CDF) of the independent random variables $X = \{X_1, X_2, ..., X_N\}$ with expectation value μ and variance σ converges to the CDF of the Gaussian distribution,[1],

$$\lim_{N \to \infty} \mathbb{P}\left(\frac{(\sum_{i=1}^{N} X_i - N\mu)}{\sigma\sqrt{N}} \leq x \right) = \frac{1}{\sqrt{2\pi}\sigma} \int_{-\infty}^{x} e^{-(x'-\mu)^2/(2\sigma^2)} dx'. \tag{2.4}$$

This result is a fundamental property of the Gaussian universality class, known as the Central Limit Theorem. As we will discuss later, it is not the only universality class that has been identified.

2.1.2 Edward-Wilkinson Universality Class

In 1981, Edward et al. worked theoretically on a random growth interface [2]. They ignored the correlations between particles and assumed that when a particle is deposited on a particular column due to gravity, it does not laterally move when other particles settle on top of it.

From this process, they showed that the growth on these kind of systems can be described as

$$\frac{\partial h(x,t)}{\partial t} = \nu \nabla^2 h(x,t) + \eta(x,t), \tag{2.5}$$

known as the Edward-Wilkinson (EW) equation. In this equation, ν is an arbitrary constant, $\nabla^2 h(x,t)$ term describes the lateral correlation or surface diffusion, and $\eta(x,t)$ is the Gaussian white noise which forces the system to grow and fluctuate.

As discussed in the previous section, for 1+1 dimension systems Family showed that the scaling exponents are $\alpha = 1/2$, $\beta = 1/4$, and $z = 2$ [3]. The EW equation is a linear stochastic equation invariant under the following translations,

$$x \to \lambda x, \quad t \to \lambda^z t, \quad \text{and} \quad h \to \lambda^\alpha h. \tag{2.6}$$

We can find the scaling scaling exponents α, z, and $\beta = z/\beta$ by re-scaling the EW (equation 2.5) equation according to the equation 2.6,

$$\lambda^{\alpha - z}\frac{\partial h(x,t)}{\partial t} = \nu \lambda^{\alpha-2}\nabla^2 h(x,t) + \lambda^{-(d+z)/2}\eta(x,t), \tag{2.7}$$

This leads to

$$\alpha = \frac{2-d}{2}, \quad \beta = \frac{2-d}{4}, \quad \text{and} \quad z = 2. \tag{2.8}$$

The other method for obtaining these scaling exponents is to solve the EW equation in the Fourier space [4][5]. We can see that the growth exponent for one-dimensional systems is 1/4, differing from the 1/2 exponent of the Gaussian Universality class. We understand that surface diffusion makes a major difference in the dynamics of the surface growth phenomena.

The probability distribution of the height fluctuations is again approximately Gaussian distribution since the operators acting on the height are linear. However, those surfaces are much more physical compared to the non-diffused surfaces of the first class.

2.1.3 Kardar-Parisi-Zhang Universality Class

In the EW equation, the surface growth is along one direction despite the effect of noise and diffusion terms causing deformations on the interface. In nature, the growing process generally is not occurring along in a single direction. For example, for a spherical substrate, the surface growth is along the normal of the interface. With the Kardar-Parisi-Zhang (KPZ) equation, we can add isotropic growth in the equation thanks to the presence of the nonlinear term.

The KPZ equation was invented in 1986 to describe the surface growth [6]. In their work, the authors gave the values of 1/3 and 2/3 for the scaling exponents for surface roughness and size of the system, respectively. These scaling exponents were first introduced in 1977, in the context of the stochastic Burgers equation [7]. Also, in 1985, Family et al. [8] introduced a detailed analysis of surface roughness for the Eden model, which we will discuss later in the next chapter. The well-known KPZ equation is given below,

$$\frac{\partial h(x,t)}{\partial t} = \nu \nabla^2 h(x,t) + \lambda(\nabla h(x,t))^2 + \eta(x,t). \tag{2.9}$$

The time derivative of height function depends on three factors: the diffusion term $\nabla^2 h(x,t)$, noise term $\eta(x,t)$ commonly chosen as Gaussian white noise, and in addition to the EW equation, we have an additional nonlinear term $(\nabla h(x,t))^2$ which describes the growth speed. The constant λ and ν usually are chosen from microscopic properties of the system.

The KPZ universality class describes a wide variety of physical phenomena, such as far-from-equilibrium fluctuations, surface growth, directed polymers, stirred fluids, and particle transport. Recent works helped to introduce a non-trivial correlation of the KPZ universality class with the random matrix theory. The literature on the KPZ universality class is not limited to theoretical works revealing the non-equilibrium fluctuations and relevance to the random matrix theory. There is a growing number of experimental results [9][10][11].

There has been a significant activity to uncover the statistical properties of the KPZ equation, the formal simplicity of which belies the complexity of this task. Finally, circa 2010, the derivation of one-point statistics for the KPZ equation was reported by two groups independently [12][13]. They proved that under the scaling of time to the power 1/3, the statistics of fluctuations for the KPZ equation converges to the asymmetrical Tracy-Widom distribution, in the limit time goes to infinity, $T \to \infty$. In other words, they showed that the KPZ equation constitutes a universality class, now known as the KPZ universality class.

2.2 Growth models

Before the seminal results discussed above, discrete models describing the growth phenomena had been developed. These discrete models continue to play a significant role in developing our understanding of the statistical properties of the interfaces.

The Eden model is one of the first models describing lattice growth. In this model, we start with an occupied lattice. Next, we find the unoccupied nearest neighbor and then fill them. The statistical properties of the Eden model fit the KPZ universality class. Another model that fits in the KPZ universality class is the ballistic deposition model, in which the particle will deposit on the first part of the surface that it encounters. Beyond their basic structure, there are numerous reports on different versions of these models. Another model that we will discuss in detail in the next chapter is the restricted solid-on-solid model. We will introduce a restriction limit to this model. Accordingly, a particle will deposit on a column whose height is less than an arbitrarily chosen integer with its nearest neighbor.

The random deposition model is the simplest model, and it is a member of the Gaussian universality class. In this model, the particle is deposited on the randomly chosen site. We obtain the well-known random deposition with the surface diffusion model by adding the diffusion to the random deposition model. This model fits in the EW universality class, as we will examine in the next chapter.

Chapter 3

Discrete Models for Describing Surface Growth

3.1 Random Deposition Model

The random deposition model is the simplest growth model. In this model, a site is chosen randomly across the interface, and a particle moves in one direction towards the chosen site and sticks to the top of that column. As shown in figure 3.1, particle B is deposited on the top of a randomly chosen column or an empty site. In this model, there are no correlations between particles [14].

The random deposition model's statistics are best described with the Gaussian universality class. As discussed in the previous chapter, Family report a detailed analysis for the surface roughness [8]. The surface roughness was calculated per seed site for various number of particles (L) with different deposition rate (M) as

$$\sigma_L(M) = \left[\sum (h_i - h(M))^2 \right]^{\frac{1}{2}}. \tag{3.1}$$

Here, $\sigma_L(M)$ is the surface thickness where h_i is the height of ith site and $h(M)$ is the mean height. They show that for the defined ballistic deposition the mean height scales as $h(M) \sim M^{\nu}$ where for the surface thickness the exponent is different $\sigma_L(M) \sim M^{\nu'}$ (the relation is not valid for too large M values). They numerically found the ν and ν' values are near to 1 and 0.30. From the combination of the numerical results they defined a finite-size scaling expression for the surface thickness as

$$\sigma_L(M) \sim L^{\beta} f(M/L^{\gamma}), \tag{3.2}$$

Where here $f(x)$ is a scaling function described as

$$f(x) = \begin{cases} x^{\nu'}, & \text{for } x \ll 1 \\ \text{Constant}, & \text{for } x \gg 1, \end{cases}$$

and $\gamma = \beta/\nu'$. Numerical results for α, β and γ respectively calculated as 0.30, 0.42 and 1.40.

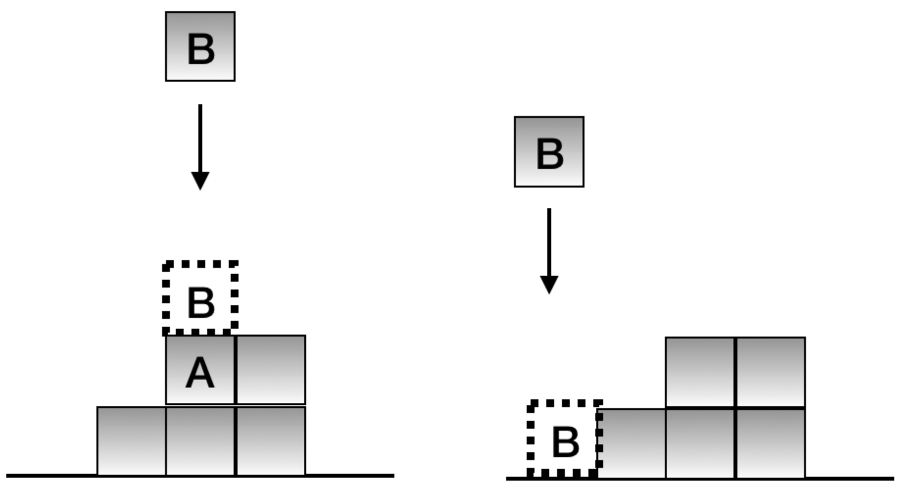

Figure 3.1: Random deposition model

3.1.1 Simulation Methods

We followed the following steps for simulating the random deposition model:

1. Firstly, we define our initial condition as a horizontal line with the length of the size of the system, N_x.

2. In each time step, new particles arrive at the interface with a constant rate of $10\%N_x$.

3. Using the permutation group, the columns which particles will fall on are chosen in each time step.

4. The process of deposition continues for a chosen time step and then we repeat the whole simulation procedure for an arbitrarily chosen number of runs, N_r.

3.1.2 Results for the Beta Exponent

The evolution of interface through time is shown in figure 3.2. The statistical properties of the interface are calculated starting with computing the scaling exponent β from the width versus time graph shown in figure 3.3. The simulation parameters are the size of the system $N_x = 10000$, time steps $N_t = 2000$, and number of runs $N_r = 100$.

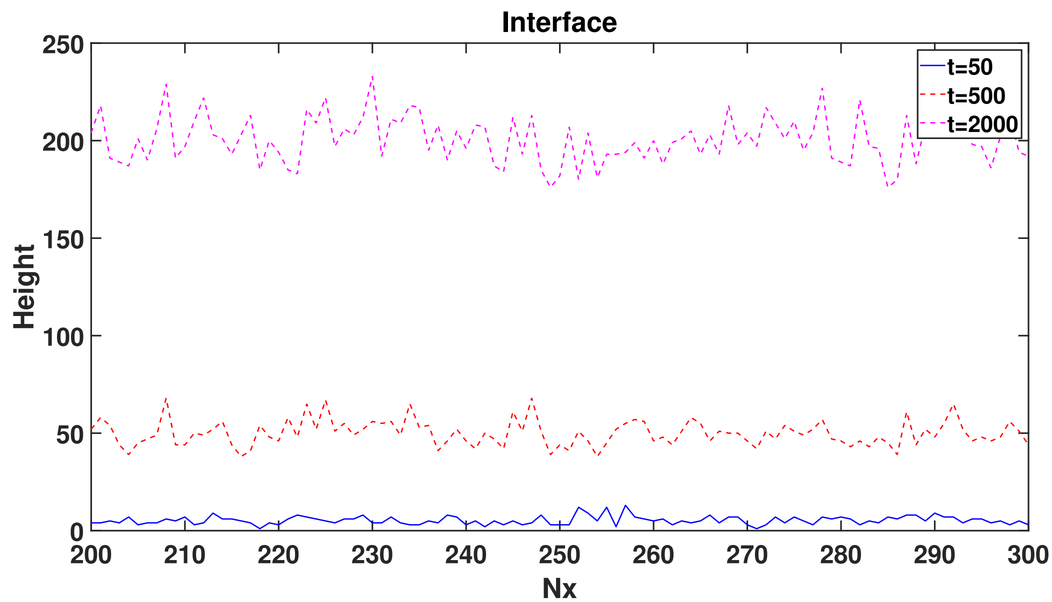

Figure 3.2: Interface for 3 different time.

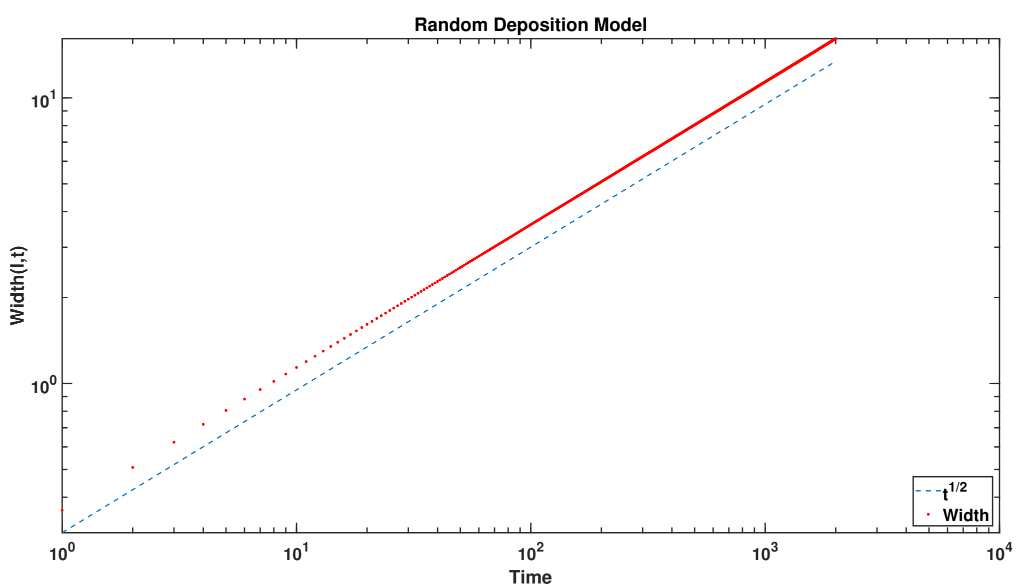

Figure 3.3: Width vs Time graph.

The value of β is calculated as 0.50 from figure 3.3 which is the expected value for the Gaussian universality class.

3.1.3 Results for Spatial Fluctuations

In order to clarify to which universality class our model fits, in addition to calculating the scaling exponent β, we can also check the statistics of the height fluctuations. As we discussed before, the height fluctuations should follow the Gaussian universality class for the random deposition model. The height fluctuations can be calculated as

$$q(x,t) = \frac{h(x,t) - \bar{h}(x,t)}{\sigma(x,t)}, \tag{3.3}$$

where $\bar{h}(x,t)$ is the mean height, and $\sigma(x,t)$ is the standard deviation. The probability distribution of height fluctuations is shown in figure 3.4 . The 3^{rd} and 4^{th} cumulant values are calculated as 0.062 and 2.998, simultaneously. The approximated value for skewness and kurtosis for the Gaussian distribution are 0.0 and 3.0.

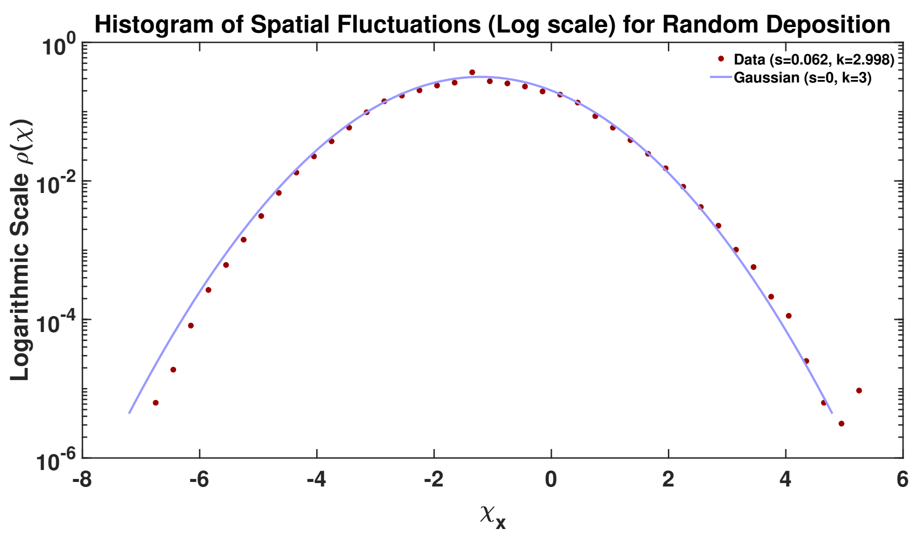

Figure 3.4: Histogram of spatial height fluctuations.

3.2 Random Deposition with Surface Diffusion Model

In 1986, Family introduced a modified random deposition model (RDSD), which contains a correlation between particles so that the particles move towards a randomly chosen site i. In addition, they are deposited according to the nearest neighbor columns. This deposition is such that the particles will stick to the column with a minimum height between columns $i-1$, i, $i+1$, as shown in the figure 3.5 [15].

There are several reports on modifying the random deposition (RD) and random deposition with surface diffusion (RDSD) models Baisakhi et al. [16] expand the correlation length starting from $N_d = 1$ which is the original RDSD they report that beyond correlation length $N_d = 3$ the surface statistical properties do not change. Another modified model was introduced by M. Horowitz et al.[17] which brings in a model containing both RD and RDSD models with probability p and $1-p$ respectively. They also numerically evaluated the scaling exponent β for different values of p.

3.2.1 Simulation Methods

For the incorporation of diffusion phenomena into the simulation, we need an additional step. Commonly, the implementation is as follows. The height of the neighboring column on the right side is checked. The falling particle will be deposited on the column which has the lower height. If both columns are of the same height, the particle will be deposited with equal probability on the chosen column or the right nearest neighbor.

Here are the steps that we followed:

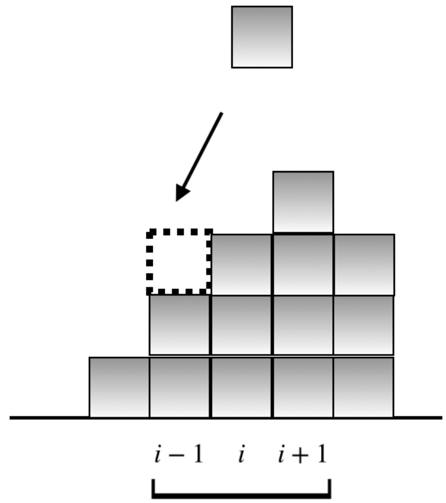

Figure 3.5: Random deposition with surface diffusion model. Incoming particle will stick to the site with minimum height.

1. The first step, as discussed in random deposition simulation, is defining the initial value for the height, $h(x, 0) = 0$. In other words, we placed N_x particles at zero initial height value.

2. Similarly to the random deposition simulation, for choosing columns that particles can fall onto, we use random permutation. In each time step, we select $10\% N_x$ columns.

3. For each particle, we check the nearest neighbors of the selected column. If the heights are all different, the particle will be deposited on the column with the minimum height. If the right and left columns have the same height as the chosen column (all heights are equal), the particle will deposit on any of them with equal probability. If any of the two columns are lowest and equal in height, the particle will deposit with a probability of 1/2 (equal probability) on any of these two columns.

4. This process continues for N_t time steps for each run. Then, these runs are repeated for N_r times.

3.2.2 Results for the Beta Exponent

As discussed in the previous chapter, for the RDSD model, we expect that the statistical properties of the model fit in Edward-Wilkinson universality class. Hence, the surface roughness changes with respect to time as $t^{1/4}$. In figure 3.7 the graph of evolution of width with respect to time is shown in logarithmic scale for a total time $N_t = 2000$, size of the substrate $N_x = 10000$, with constant deposition rate of 1000, and for 100 different realization of disorder. The interface for a single simulation for 3 different times is plotted in figure 3.6. As we can see, the interface is obtained as a result of the diffusion in comparison to the random deposition simulation shown in figure 3.2. Our result is in good agreement with the expected analytic results as shown in figure 3.7.

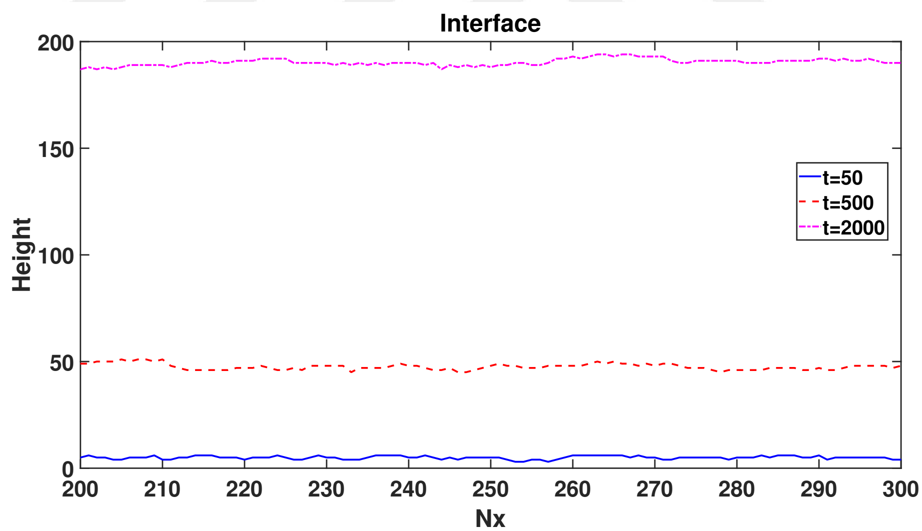

Figure 3.6: Interface for 3 different time steps.

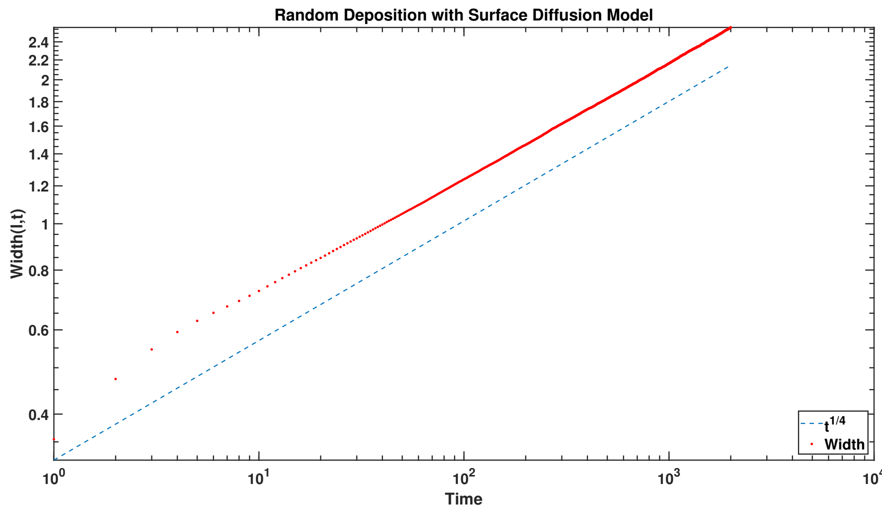

Figure 3.7: Change of width with respect to time.

3.2.3 Results for Spatial Fluctuations

From the spatial fluctuations of the interface calculated as 3.3 as expected for such random growth, the probability distribution for height fluctuations should follow the Gaussian distribution. The histogram of spatial fluctuations in logarithmic scale is shown in figure 3.8, the values for 3^{rd} and 4^{th} cumulants are calculated as 0.00 and 3.02, which are in good agreement with the Gaussian distribution.

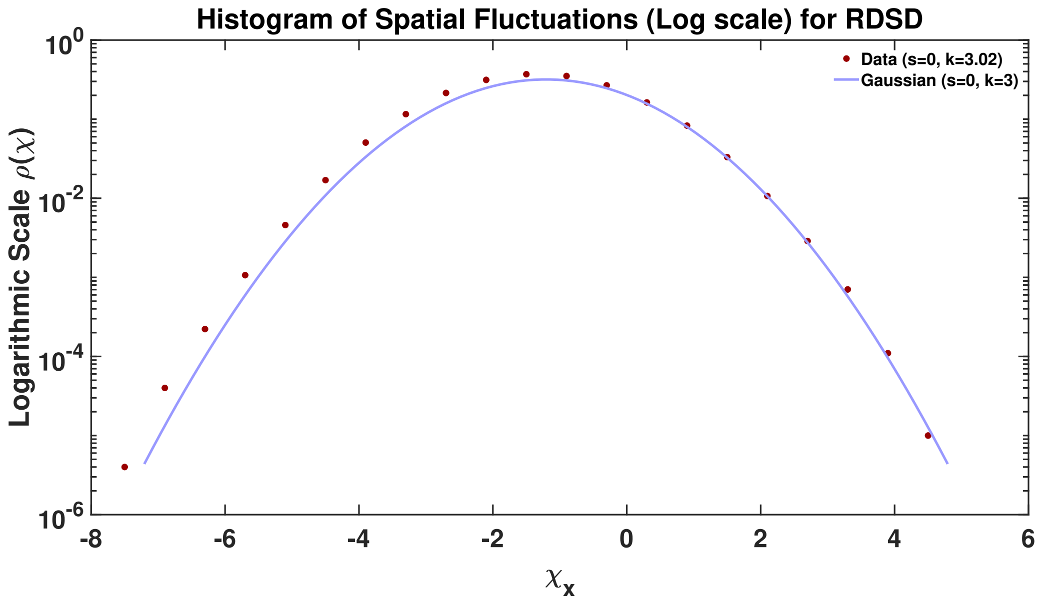

Figure 3.8: Change of width with respect to time.

3.3 Ballistic Deposition Model

The ballistic deposition model was first introduced by Marjorie J. Vold [18] as a numerical approach to the problem of sediment volume for spherical particles. Their model was physically described as follows. The particles are randomly distributed homogeneously over a large volume. Due to gravity, each particle falls and sticks rigidly to the bottom or onto the previously dropped particles. There are several modifications to the ballistic aggregation model to increase the physical realism of this deposition model [19][20]. Several simulations were also introduced based on this model [21][22].

Aggregation formation in the growing processes attracted significant attention due to their wide variety of phenomena and their scaling behavior in experiments, theories, and numerical observations. A seminal work on the scaling behavior of the ballistic deposition model was by F Family [8] [3], who focused on the thickness of the interface. Examination of the ballistic deposition model on a square lattice with periodic boundary conditions was implemented in the following way:

1. A horizontal line consisting of N particles is defined as the initial condition.
2. A site above this initial interface is chosen randomly, and a particle is placed on the chosen site.
3. The particle in step 2 moves vertically towards the chosen site until it sticks to the nearest neighbor (NN) on the initial line.

As discussed before, the KPZ model was introduced in 1986 [23]. This is a continuous model based on a nonlinear partial differential equation describing the lateral growth. The scaling exponents turn out to be close to those obtained by F Family [8][3]. There are several papers connecting the KPZ equation to the ballistic deposition model [24][25]. In 1998, T. Nagatani reported a direct connection between the ballistic deposition and KPZ equation by reproducing the KPZ equation in $1 + 1$ dimension from the ballistic deposition model [26].

The modified ballistic deposition models have a few variance. The original ballistic deposition model, also known as the nearest neighbor (NN) ballistic deposition model (figure 3.9)can be described as:

1. A site on the interface is chosen randomly.
2. The particle falls vertically onto the first surface that it counters (It could be on the top of the chosen site or the side of the nearest neighbor).

Another variant is the next nearest neighbor (NNN) ballistic deposition model shown in figure 3.9b which can be described as:

1. A site on the interface is selected randomly.
2. Particle falls vertically on the first corner or side or top of columns it collides with.

Another variant is the next nearest neighbor (NNN) ballistic deposition model shown in figure 3.9b which can be described as:

1. A site on the interface is selected randomly.
2. Particle falls vertically on the first corner or side or top of columns it collides with.

A further modification on the ballistic deposition model has been investigated recently[27]. In this model, they introduced a new parameter containing inter-particle forces such as Coulomb and van der Waals. In addition, they introduce a stickiness parameter that takes values from 0 to 1, 0 corresponding to non-adhesiveness, and 1 corresponding to maximum stickiness. In their work, they calculated the scaling exponents and showed that their model follows the KPZ universality class. Figure 3.10 shows the probable places that a new particle can stick.

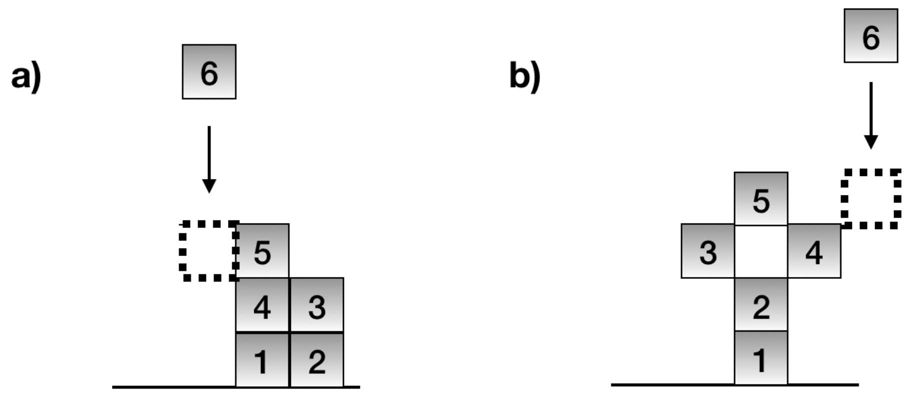

Figure 3.9: (a) nearest-neighbor (NN) ballistic deposition, (b) next-nearest-neighbor (NNN) ballistic deposition. Here the numbers show the placement time of particles.

Investigation of height fluctuations in ballistic deposition model was performed by T. J. Oliveira et al. [28] They showed that the height fluctuations of the interface exhibit the Tracy-Widom GOE (Gaussian orthogonal ensemble) distribution for flat interfaces with periodic boundary conditions.

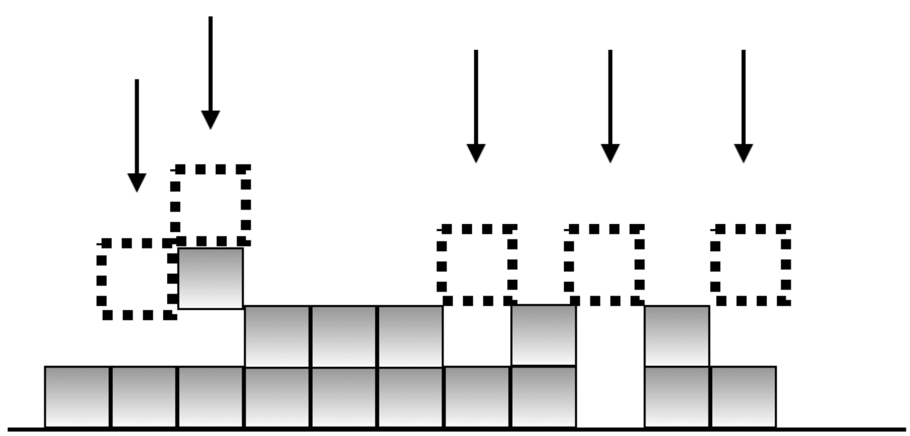

Figure 3.10: Possible places for new particles falling on the interface.

3.3.1 Simulation Methods

In this section, the simulation for the ballistic deposition model is investigated. For simulating the nearest neighbor BD in a 1D system, the steps are as follows:

1. Since we have a 1D system, the initial height is set to be a line with the length of the size of the system N_x, where the initial values of heights are zero at $t_{intial} = 0$, and $h(x, 0) = 0$.

2. In our simulation method at each time step, the quantity of the deposited particles is defined by a constant such that it corresponds to 10% of the size of the system.

3. A random permutation group is chosen within the system size to determine the columns, where the particle deposits.

4. As described in the previous section, for each particle, if the height of the chosen column j, is greater or equal than its nearest neighbors (j-1,j+1), the height of the column increases by one. Otherwise, the particle sticks to the maximum neighbor, so the new height of the column becomes the maximum height of the nearest neighbor.

$$h(x_j) = \begin{cases} h(x_j) + 1, & \text{if } h(x_j) \geq h(x_{j-1}), h(x_{j+1}) \\ \max(h(x_{j-1}), h(x_{j+1})), & \text{otherwise.} \end{cases}$$

5. This procedure is continued until arriving to the final time t_{final}, and repeating this process for a certain number (N_{run}) of times to form an ensemble of simulations.

3.3.2 Results for the Beta Exponent

In Fig 3.11 the evolution of the system with respect to time is shown. We can find the statistical properties of the system with studying the evolution of the interface in time. Starting with scaling exponents described in 3.1, as discussed in the previous chapter, the roughness of the interface is related to time as $w(l,t) \sim t^{\beta}$ where for KPZ universality class $\beta = 1/3$.

In fig 3.12 the graph of interface width with respect to time is plotted, for which the value of β is calculated as 0.29 from an ensemble of 100 simulations, with a system size of $N_x = 2100$, number of time steps $N_t = 1000$, with deposition rate $dr = 210$. The reason why our calculated result is moving away from the expected value is the thin-deep wells on the interface. We will introduce a new method to remove these wells in order to diminish the artifacts caused by the numerical applications in the next chapter .

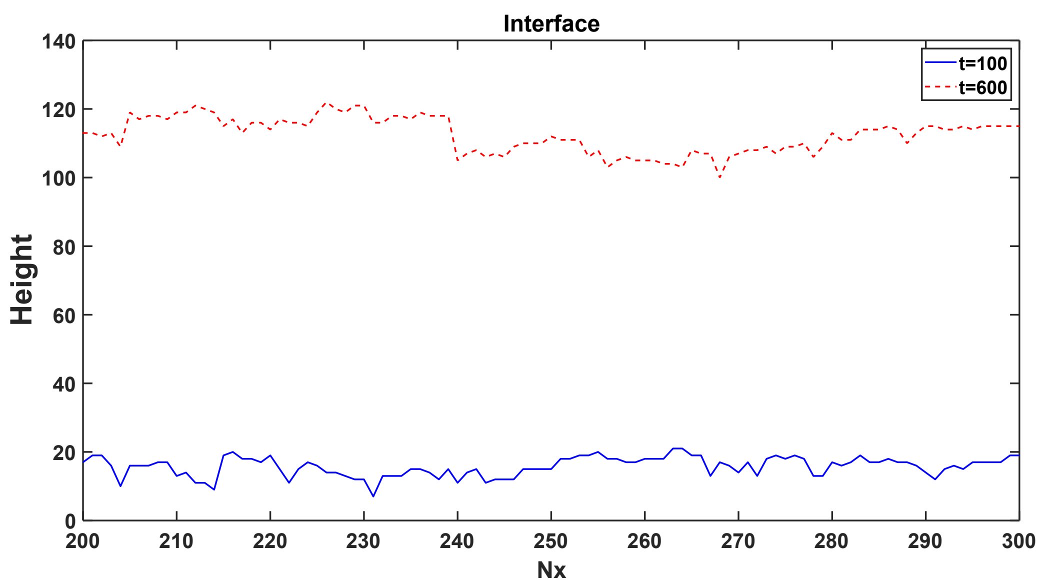

Figure 3.11: Evolution of the interface with respect to time.

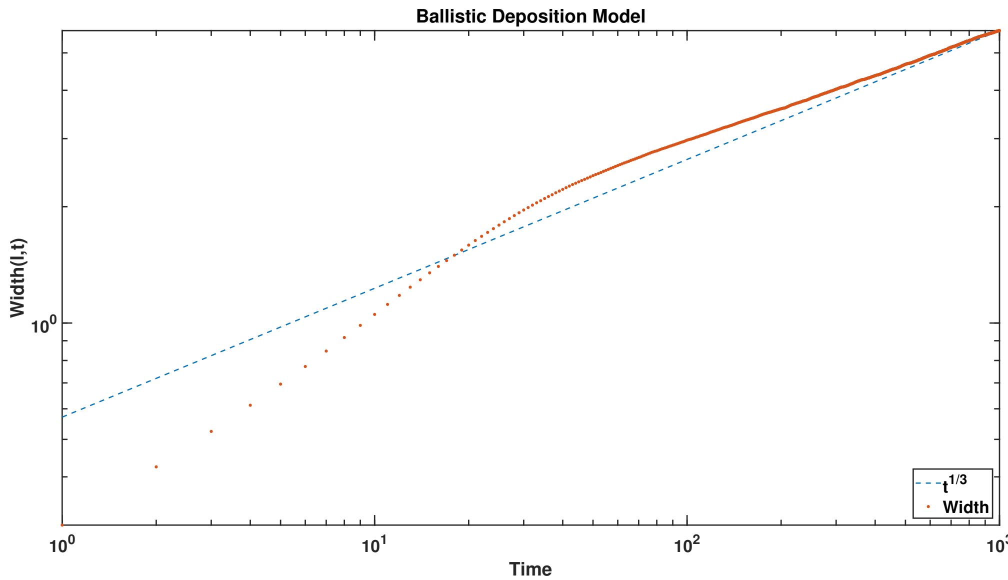

Figure 3.12: The width versus time graph.

3.3.3 Results for Spatial Fluctuations

The other way to test which universality class does our model fits is through the height fluctuations' distribution. This distribution function, for the growing processes in the KPZ universality class, should follow the Tracy-Widom GOE distribution. The height fluctuations are calculated as discussed in 3.3 Here in figure 3.13 we can see the probability distribution function for height fluctuations. The 3^{rd} and 4^{th} cumulants are 0.14 and 3.13 respectively. For Tracy-Widom distribution, the skewness and kurtosis values are approximately 0.29 and 3.16. We expect that the reason for the difference between the approximated and calculated results are the same as discussed in the previous section which are the thin-deep wells on the interface.

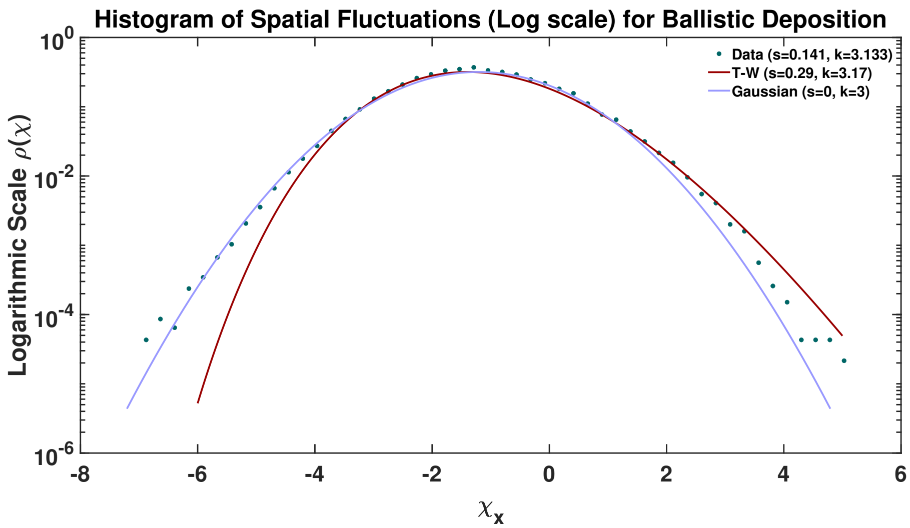

Figure 3.13: The width versus time graph.

3.4 Eden Model

In 1961, Eden introduced a two-dimensional model in biological systems, describing the growth of bacteria colonies on a flat interface [29]. The relation of interface's thickness and length was numerically investigated by Jullien, R., and R. Botet [30]. In their work, they introduce 3 different versions of the Eden deposition model in one dimensional (1D) substrate with periodic boundary conditions. On-lattice Eden A model can be described as:

1. Select all the unoccupied sites near the surface.
2. One of the unoccupied sites is chosen randomly with equal probability.
3. The chosen site is occupied by adding a new particle.

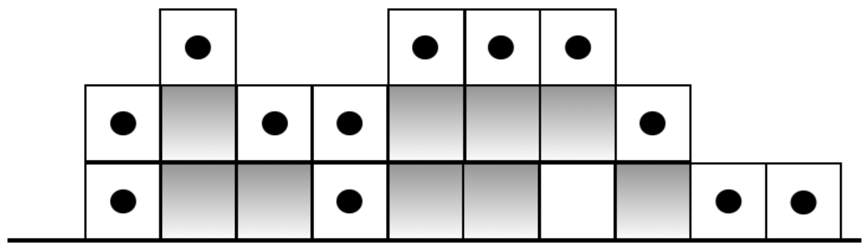

Figure 3.14: Eden A deposition model. Possible places for new particles on the interface is shown by black circles.

In Eden B model which is the original model:

1. Select all open bonds on the surface.
2. One of the open bonds is chosen randomly with equal probability.
3. Add a particle on the edge of the chosen bond.

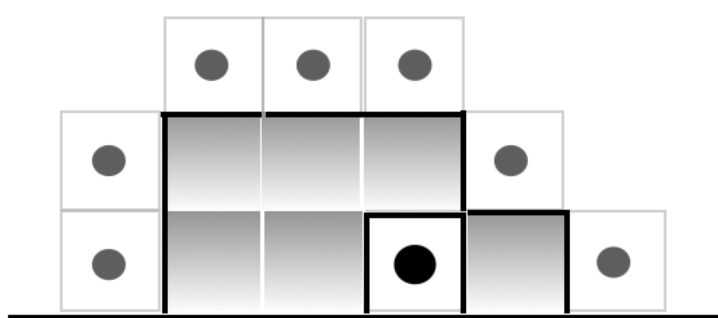

Figure 3.15: Eden B deposition model. Open bonds are shown by black lines and Possible places for new particles on the interface is shown by grey circles. In contrast to Eden A model the site with black circle can be occupied here.

Eden C version can be described as,

1. Select an occupied site of the interface.
2. An open bond connected to the chosen site is selected randomly.
3. A particle is added equiprobably on the edge of the chosen bond.

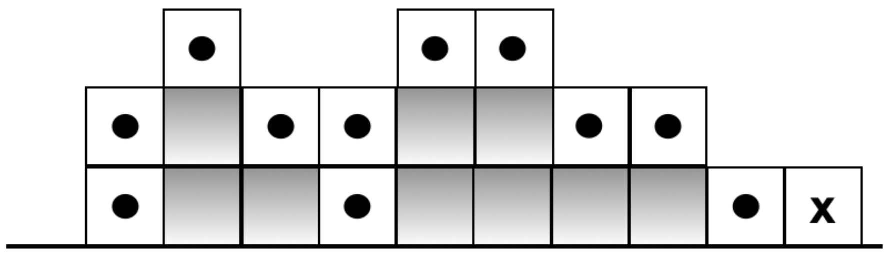

Figure 3.16: Eden C deposition model. Possible places for new particles on the interface is shown by black circles. The site with X can not be occupied in the Eden model C.

There is substantial literature analyzing the scaling exponents of the Eden model for different aggregates shapes. Jullien, R., and R. Botet [30] showed that thickness depends on the size of the system to the power $\alpha = 1/2$ for all the three versions of the Eden model in the long time range. Statistical properties of circular aggregates are investigated in the works referenced here [31][32]. They showed that the exponents α and β are 1/2 and 1/3, respectively, which are the characteristic dependencies of the KPZ universality class. In addition, they showed that the one-point height fluctuations follow the Tracy-Widom GUE (Gaussian Unitary Ensemble) distribution [33] [34] [35].

3.4.1 Simulation Methods

We chose the Eden C model as the basis for our calculations. The simulation steps are as follows,

1. The first step, as discussed for other models, is to define the initial condition.Instead of 1D setting, here we define our initial condition in 2D system consisted of N_y and N_x standing for the maximum height and number of particles, respectively. Hence, the dimension of the system is defined as $N_y N_x$. In the defined 2D system, the first height for all of particles is set to 1 (the first row of matrix for all columns is equal to 1).

2. The second step is to find the empty sites on the system, and hence, we define a mask which consists of the empty sites of the system. By multiplying the mask with the first initial matrix, we guarantee that the particles will not fill the same site.

3. After filtering the filled sites, we know the available sites that can particles fill in. Then, we take a random permutation of them and choose a certain number of sites with respect to our deposition rate which is chosen to be $10\% N_x$.

4. Afterwards, we get the coordinates of the possible sites so that we can fill them later.

5. As discussed in the previous section, the surrounding of the new coordinates that will be filled are marked as possible sites while respecting the boundaries of the system.

6. A new mask is created with respect to the new particles deposited, so that our possible sites are renewed. The maximum number of possible places is equal to the deposition rate for each time step.

7. Algorithm is iterated for the number of time steps and experiments, N_t and N_r.

3.4.2 Results for the Beta Exponent

The statistical properties of the system are examined, starting with the calculation of the β exponent. As discussed in the previous chapter, we expect that the statistical properties of the Eden model should fit in the KPZ universality class. In figure 3.17 the evolution of width with respect to time is shown. The scaling exponent β is determined as 0.3060 using a fitting method which is in good agreement with the value of 1/3, expected from the analytical calculations.

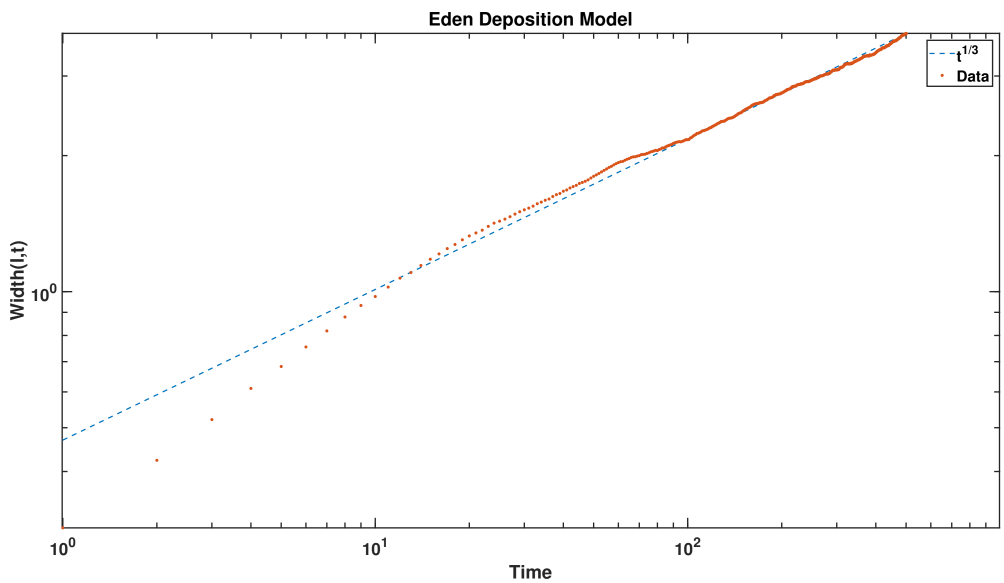

Figure 3.17: Width with respect to time graph for Eden model.

3.4.3 Results for Spatial Fluctuations

In this section, the statistical properties of the interface and the belonging universality class are discussed. The second property we studied is the characteristics of the spatial fluctuations. The spatial fluctuations are calculated based on the equation 3.1. In figure 3.21 the PDF of height fluctuations is shown. The results are in good agreement with the TW GOE distribution. The skewness and kurtosis values are 0.238 and 3.029, respectively.

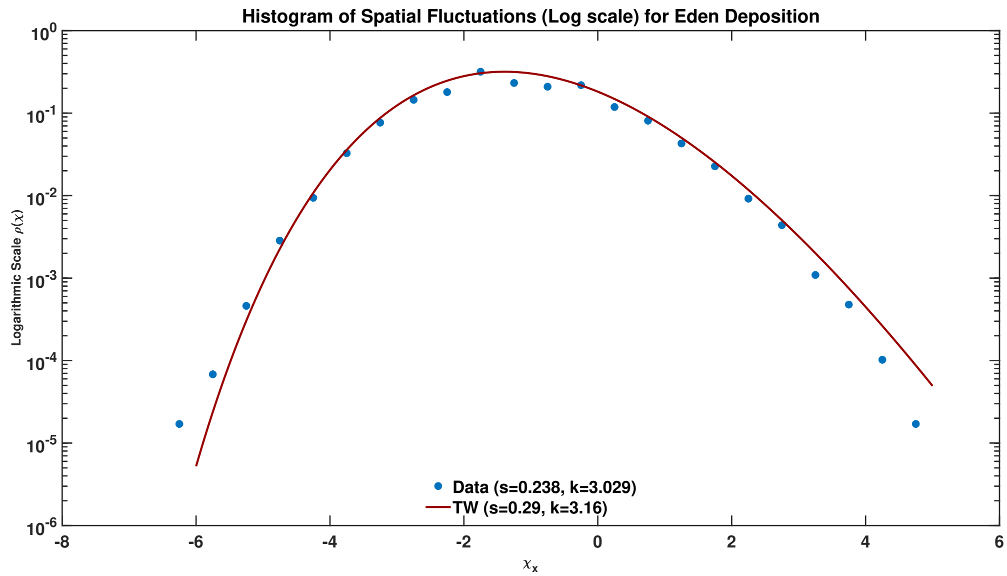

Figure 3.18: Histogram of fluctuations for the Eden C model.

3.5 Restricted Solid-on-Solid Model

The Restricted Solid-on-Solid model (RSOS) was introduced by Jin Min Kim and J. M. Kosterlitz in 1989. They showed that the RSOS model results similar to the expected KPZ universality class for a relatively small-sized system.

In the RSOS deposition model, particles are deposited randomly on a flat surface. Still, their deposition is restricted in a way that the height difference between nearest neighbors should be less than a particular integer.

$$| h(x) - h(x') | \leq N, \tag{3.4}$$

where x' is the position of nearest particle and N is an arbitrary integer.

There are several works on the statistical properties of the RSOS model. In [28] they examined the roughness exponent, correlation function, and height fluctuations, they showed that the width grows with time as $t^{1/3}$, that correlation function is in a good agreement with the Airy process [36], and height fluctuations follow the Tracy-Widom GOE (Gaussian orthogonal ensemble) distribution.

3.5.1 Simulation Methods

For simulating the RSOS model, the critical point is to add a restriction property to the simulation. Here are the steps followed in the simulation process:

1. The first step, as discussed in the last 4 models, is to define the initial values for height. For 1D system the initial height is defined as $h(x, 0) = 0$, it seems like that we initially placed particles at zero height. The length of the system is then equal to the number of particles.

2. The second step is to randomly choose columns which in each time step particles can fall onto them. The process of randomly choosing columns is done by random permutation as discussed for previous models. For each time step we set the deposition rate at $10\% N_x$.

3. Add this step we need to add the restriction. The logic behind this step is that for each particle in each time step, we check that if the height difference between neighbors is less than 1 the particle is deposited on the column else, the particle will not be deposited on the column.

4. The simulation will proceed for N_t time steps and repeated for N_r times.

3.5.2 Results for the Beta Exponent

In RSOS model the small restriction that we introduced has remarkable effects on the scaling exponents and statistical properties of the interface.

Starting with the interface appearance in figure 3.19 we can see a smooth interface in contrast with the other models mentioned in this chapter. The statistical properties of the interface can also be examined, beginning with the surface roughness scaling exponent.

The simulation is performed for $N_x = 24000$ particles, $N_t = 2500$ time steps, and for $N_r = 100$ different realizations of disorder. In figure 3.20, the graph of width is shown with respect to time, it is evident that the simulation data are in good agreement with the expected analytical result for the KPZ universality class.

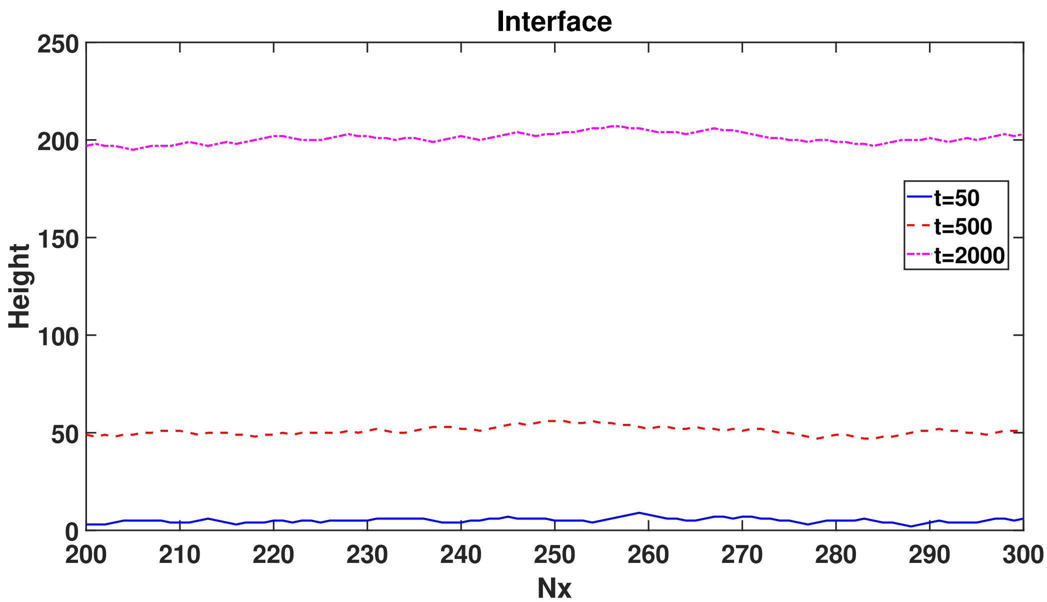

Figure 3.19: Interface for 3 different time steps.

3.5.3 Results for Spatial Fluctuations

In this section, the statistical properties of the interface and the belonging universality class are discussed. The second property we studied is the characteristics of the spatial fluctuations. The spatial fluctuations are calculated based on the equation 3.1. In figure 3.21 the PDF of height fluctuations is shown. The results are in good agreement with the TW GOE distribution. The skewness and kurtosis values are 0.285 and 3.174, respectively.

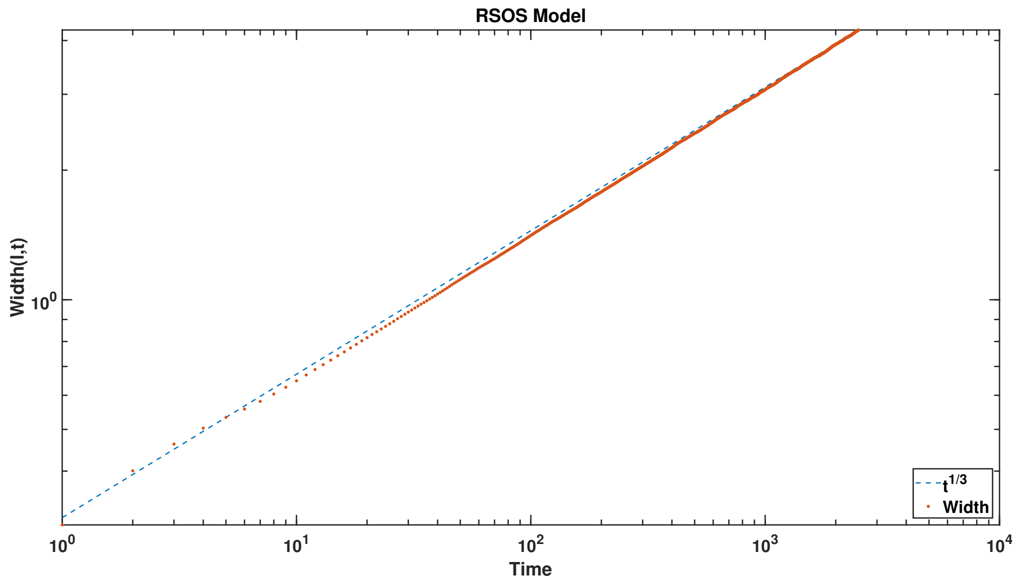

Figure 3.20: The width versus time graph.

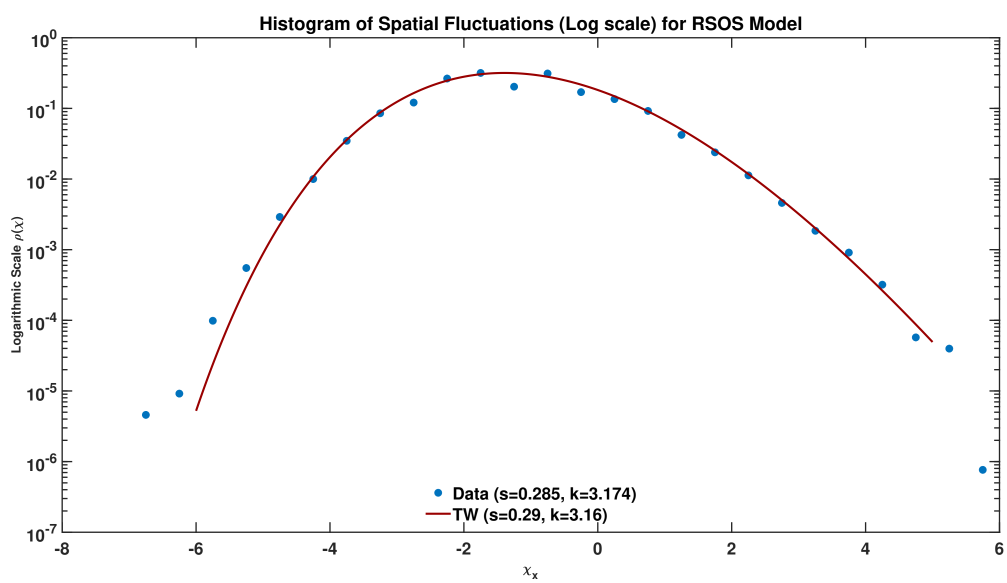

Figure 3.21: The histogram of fluctuations.

3.5.4 Physical Interpretation and Comparison of the Discrete Models

In this chapter, we started with the simplest model describing the surface growth phenomena, namely, the random deposition model. In this model, the particles are deposited on randomly chosen columns on the interface. One can trivially infer why this model fits in the Gaussian universality class, given that each site evolves independently of all others. More realistic modeling requires the inclusion of diffusion, particle-particle interactions, interactions with external forces, and, most importantly, nonlinear behavior. Moving one step forward in realism, we can add a diffusion term, which tends to smoothen the interface. The effect of the diffusion term on the interface can be seen directly in figure 3.6 in comparison with figure 3.2.

In both the random deposition and random deposition with surface diffusion models, the crucial factor for the complex behavior of the growth phenomena in nature is missing, namely, nonlinearity. The ballistic deposition, Eden, and restricted solid-on-solid models add this crucial ingredient. The Eden model specializes in lattice growth, while the ballistic deposition and RSOS models describe the surface growth phenomena. In the ballistic deposition model, the deposition process depends not only on the chosen column but also on its nearest neighbor. As a thought experiment, consider a system with sticky particles. When a particle moves toward a column, it can stick to its nearest neighbor before reaching the surface of the chosen column. The described stickiness can be a friction between 2 particles or particle-particle forces like coulomb or van der Waals forces. As an example, one can think of snowflakes falling on the windshield of a car.

The RSOS model, in comparison to the ballistic deposition model, introduces mainly a computational novelty rather than one of a physical nature. In this model, we restrict the height difference between columns which smooths out the peaks on the interface. This results in an improvement of the diffusion effect in comparison to the ballistic deposition model. The numerical supremacy of the

RSOS model can be directly seen from our results in section 3.5. To improve the ballistic deposition model numerically and physically, we try to introduce new methods in the next chapter.

Chapter 4

Modifications on the Simulation Methods for the Interface Statistics

4.1 Binning Method

In the previous chapter, we discussed discrete models describing the surface growth phenomena. We simulated these models and tested the universality class in which they fit in. Although our numerical results were approximately close to the expected results, there are several ways to improve our numerical methods.

Recently, in 2014, Sidney G. Alves et al. [**?**] proposed a new numerical method for calculating the statistical properties of the interface for the ballistic and grain deposition models. In this chapter, we apply their methods for the ballistic deposition model and introduce a new method similar to the binning method.

In the binning method, we split the interface into bins with arbitrary size (ϵ) in each time step. As mentioned in the previous chapter, there are some undesirable thin-deep wells on the interface. The binning method helps to minimize these holes on the interface by using the maximum height inside each bin. We only apply this method for statistical calculations. Hence, the physical properties of the system are not affected.

4.2 Simulating Ballistic Deposition Model with the Binning Method

Particularly in growing systems following the ballistic deposition model, we get some narrow-deep wells that cause a variance in the interface forcing the results out of the universality class. The same numerical method we explained in section 3.3.1 is used for simulating the ballistic deposition model. Still, in addition, we divide the interface into bins with size ϵ, in each time step. We choose 6 different values for $\epsilon = [1, 2, 3, 4, 5, 6]$, where $\epsilon = 1$ stands for the common method we used in the previous chapter.

4.2.1 Results for the Beta Exponent

We performed the simulation for the number of particles $N_x = 24000$, for a total time steps $N_t = 2500$, with deposition rate $d_r = 2500$, and repeated for $N_r = 100$ number of runs. In figure 4.1 the interface in a particular time is shown for 6 different ϵ values. It is evident that the binning method has helped achieving a smoother interface by minimizing the thin-deep wells on the interface.

The scaling exponent β is obtained from the interface roughness with respect to time graph shown in figure 4.2 for 6 different values of ϵ. As the picture illustrate, increasing the ϵ causing faster convergence to the analytical expected value for the β exponent. The β scaling exponent values for different ϵ values are summarized in table 4.1.

From table 4.1 improvement regarding the binning method can be remarkably

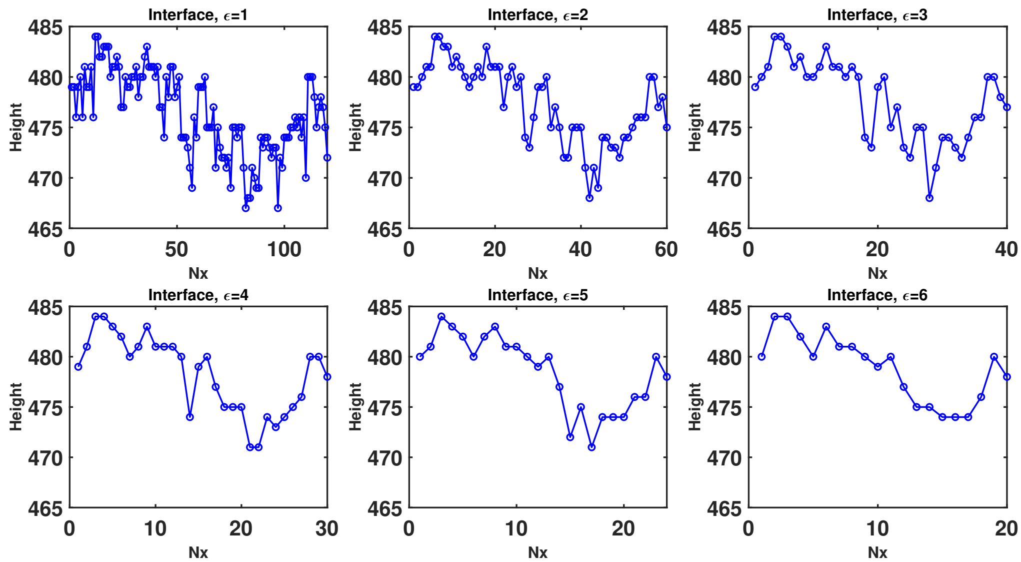

Figure 4.1: Interface view for 6 different ϵ values.

ϵ	β
1	0.297
2	0.325
3	0.3330
4	0.3430
5	0.341
6	0.342

Table 4.1: The β values calculated for 6 different ϵ using fitting method.

seen. In $\epsilon = 3$ we got our best result for scaling exponent β.

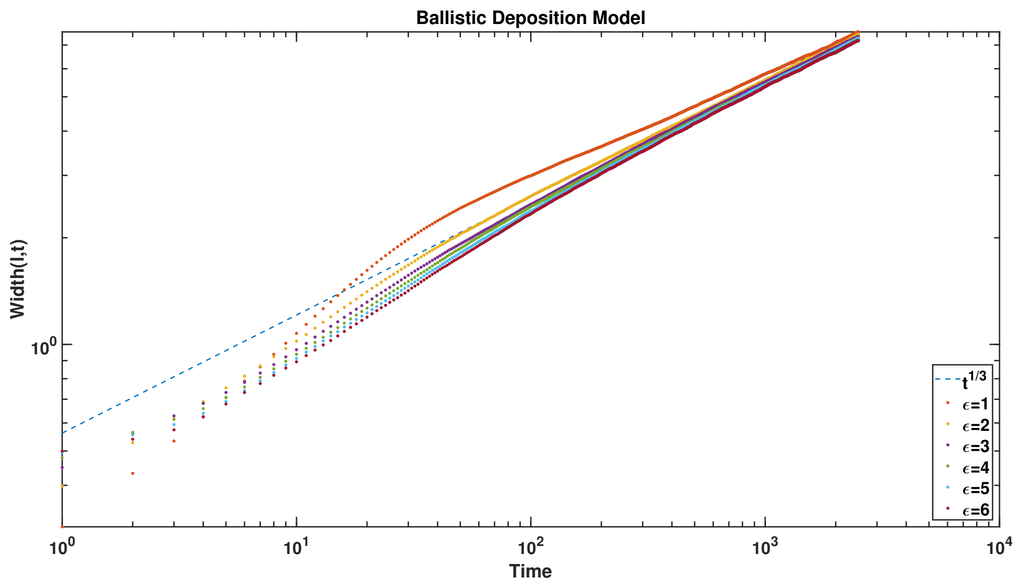

Figure 4.2: The width with respect to time graph for 6 different ϵ values.

4.2.2 Results for Spatial Fluctuations

The height fluctuations were calculated using equation 3.1. The PDF of height fluctuations is shown in figure 4.3 for different ϵ values. As depicted in 4.3, for $\epsilon = 1$ the skewness and kurtosis values are obtained as 0.0202 and 3.105, respectively. On the other hand, the skewness=0.233 and kurtosis=3.137 for $\epsilon = 3$ show the improvement for our numerical results, which are in good agreement with TW GOE distribution's values. The effect of binning method can be remarkably seen from both the beta exponent and the PDF of height fluctuations. The results we obtain match the expected results for the KPZ universality class.

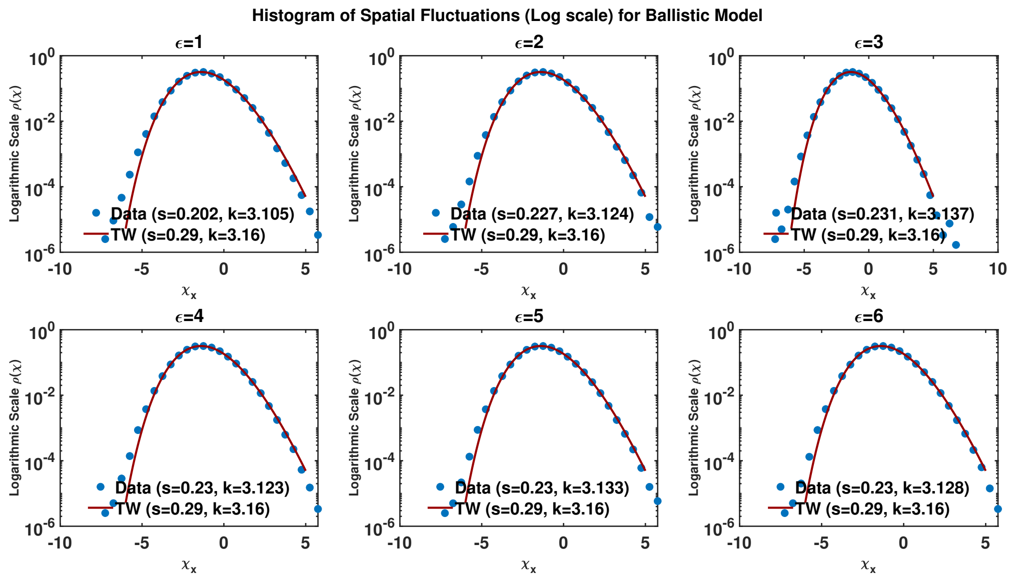

Figure 4.3: The histogram of fluctuations for 6 different ϵ values.

4.3 Restriction Factor Method

We present a new method for decreasing the effect of thin, deep wells on the interface. Our method essentially follows the binning method described at the beginning of this chapter with small modifications. In this method, we calculate the difference between the heights of each column and the mean height of the interface in each time step. If the difference is less than an negative arbitrary integer, the height of that column is set equal to the mean height.

$$h(x,t) - \bar{h}(x,t) < -RF \tag{4.1}$$

Here the RF is the arbitrary constant acting as a restriction factor. With this method, we can eliminate the holes present in the interface by eliminating the least amount of information from the interface.

Although the appearance of the undesirable holes is uncommon, they cause a major problem in the correct evaluation of the statistical properties of the system. The restriction factor method improves this issue by detecting holes on the interface, which is the essential feature that the binning method lacks. In addition, when we have a deep hole on the interface, the probability that a particle can fall to that hole is almost zero due to the nature of the ballistic deposition model.

There are two distinct approaches to this problem. The first is to deactivate that column which means that we exclude that column from the system. This approach would affect the size of the system, so it cannot be a viable solution. The second approach is the restriction factor method which, instead of eliminating the columns from the system, replaces them with the average height. This helps to improve the information integrity of the system.

4.3.1 Results for the Beta Exponent

The initial conditions used in this simulation are the following:

- The number of particles or size of the system is $N_x = 24000$,
- number of time steps $N_t = 2500$,
- number of particles falling in each time step or deposition rate is $dr = 2400$,
- repeating the simulation for $N_r = 100$ number of runs.

An arbitrary subsection of the interface is shown in figure 4.4. For examining the effect of the restriction factor method, three different RF values were tested. As it can be seen in the top right corner graph of figure 4.4, with the $RF = 7$, we get an unrealistic representation of the interface. Almost all of the points are moved toward the average. In contrast, if we increase the restriction factor too much, we almost have no effect on the interface as in the case for restriction factor 21 in figure 4.4. Due to these, the best results were found between these values. In this example, it is chosen to be 14. This gives the most realistic interface that deals with the issue of the unfavorable and unrealistic holes in the ballistic deposition model.

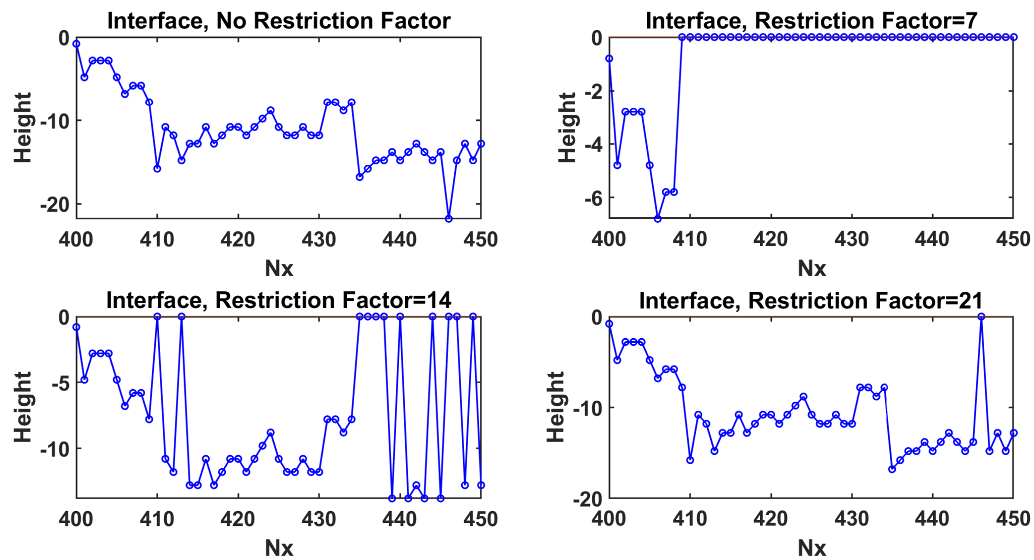

Figure 4.4: Interface height for no restriction facetor and restriction factor equal to 7, 14, and 28.

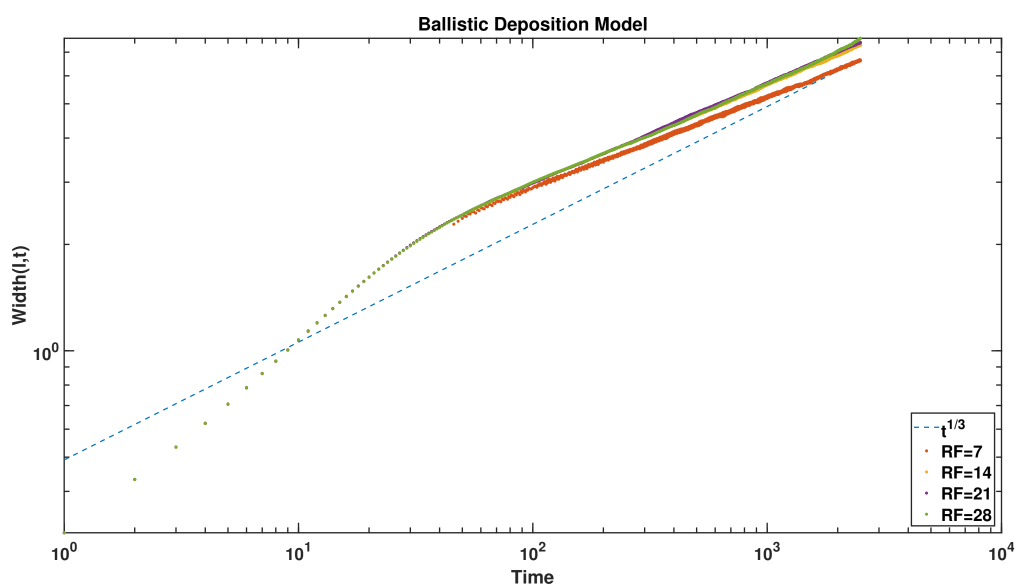

Figure 4.5: Width with respect to time.

RF	β
7	0.2640
14	0.2830
21	0.2980
28	0.2980

Table 4.2: The β values calculated for 4 different restriction factor (RF) using fitting method.

The β exponents are calculated from width time graph 4.5 using linear fitting method. The β values are listed in the 4.2 table. When the restriction factor is increased too much, the result is almost the same as the unmodified simulation. In the low restriction factor case, the beta exponent deviates from the expected value since we excessively average our information on the interface with a low restriction factor. The most reasonable results that agree with the initial beta exponent of the system are restriction factors of 14 and 21, as it can be seen from the figure 4.5 and table 4.2. We can further consolidate the results of the effectiveness of the restriction factor method by examining the other statistical properties of the system.

4.3.2 Results for Spatial Fluctuations

Another way to classify the universality class is through the examination of height fluctuation distribution. The height fluctuations were calculated as described in the previous chapter, and the histogram for the four different restriction factor values that are mentioned above are plotted. As it can be seen from figure 4.6, in two extreme cases (low and high restriction factor), we have a large deviation from the expected skewness and kurtosis value of TW GUE distribution, as can be seen in figure 4.6. The best result was shown to be for restriction factor 14, and there is a reasonably close result for restriction factor 21. In the PDF of fluctuations, there is a left tail behavior that appears to arise from eliminating some of the negative height fluctuations. These results agree entirely with the previous results of the beta exponent and the representation of the interface. The results of figure 4.6 clearly show the validity of the restriction factor method. But, one question remains, is it a better method than the binding method?

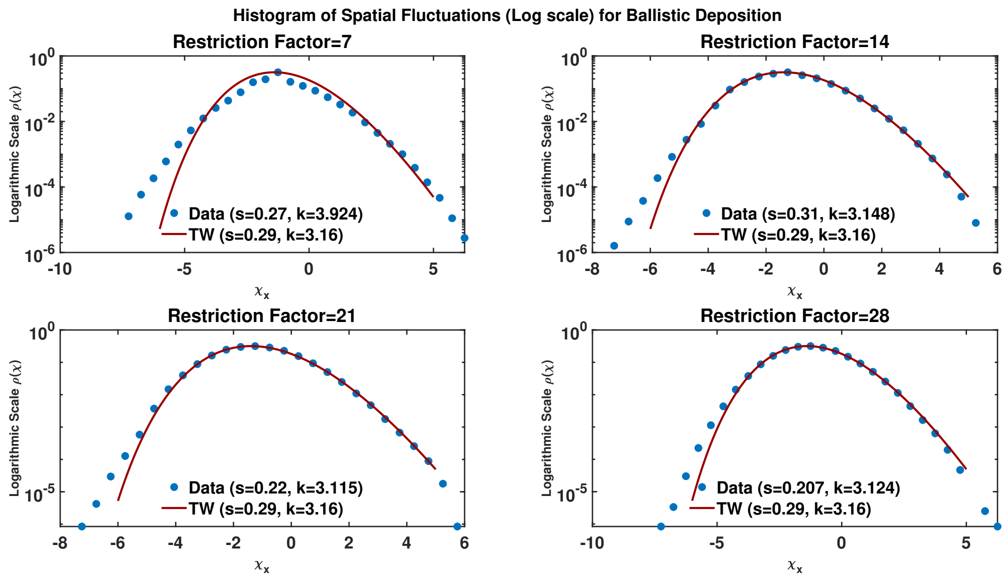

Figure 4.6: Histogram of height fluctuations.

4.4 Comparison of Binning Method with the Restriction Factor Method

Both the restriction factor and the binning methods were shown to improve the results numerically. In the binning method, the suggested alteration was only on the calculation of statistics of the system and not on the core procedure of the model itself. This sole change of the calculation method did not reflect the problem of deep holes, which is a drawback of the deposition model. Compared to the binning method, the proposed restriction factor method better reflects the lateral growth of the system, which averages out the deep holes.

1

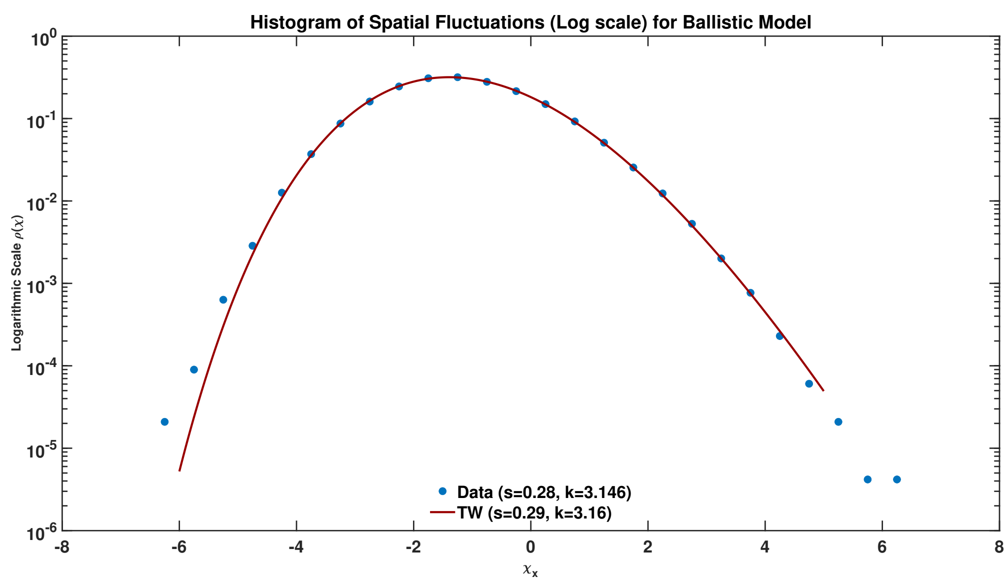

Figure 4.7: Histogram of height fluctuations for binning method, $\epsilon = 5$ with number of runs $N_r = 200$.

1

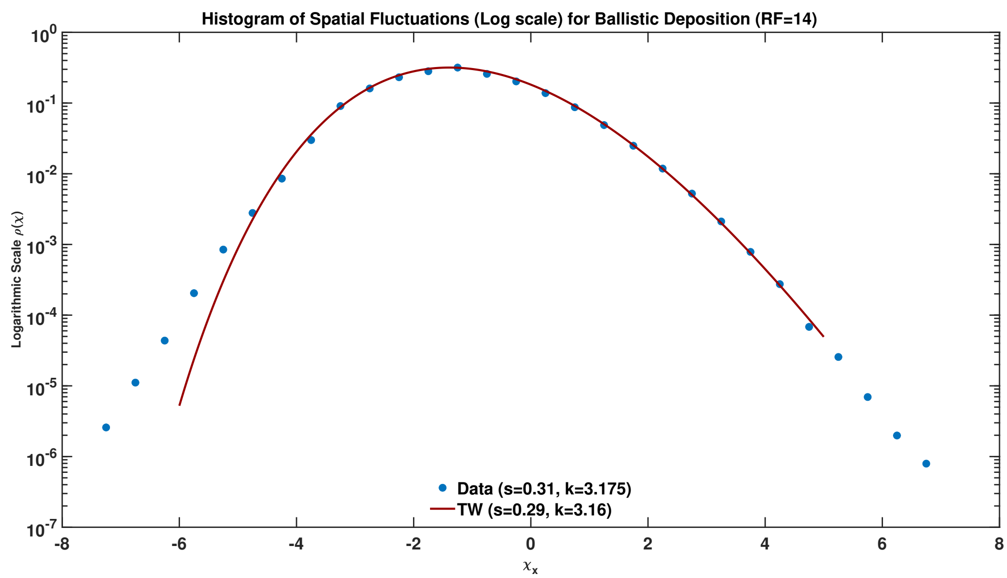

Figure 4.8: Histogram of height fluctuations for restriction factor method, $RF = 14$ with number of runs $N_r = 200$.

Comparing the restriction factor and the binning methods, they both showed physical and numerical improvements in the statistical properties of the system. The results obtained were unstable due to the finite disorder realizations. The minimization of the insatiability process can be overcome by increasing the number of experiments (it corresponds to increasing the number of runs in simulations).

In the previous sections, from statistical analysis of binning and restricted factor methods in figure 4.3 and 4.6, the best results were obtained in $\epsilon = 5$ and $RF = 14$. These results are further examined in figure 4.7 and 4.8 by observing the PDF of height fluctuations for 200 different realizations of disorder. Increasing the number of runs helps to diminish the artifacts of the finite experimentation. From the obtained results, the skewness values for the binning and restriction factor method are 0.28 and 0.31, and the kurtosis values are 3.146 and 3.175, respectively.

Overall, the RF method gives better results in comparison to the binning method. The reason behind this is that the restriction factor method helps to average out the unrealistic holes on the interface, which lowers the variance of the height distributions and therefore increases the skewness and kurtosis of the system. Since the value of the holes is set to be equal to the mean height in contrast to the binning method, where the holes are set to the maximum of neighbors, variance in the restricted factor method decreases much more rapidly than the binning method. The abovementioned reasons conclude that the RF method has significant numerical and physical advantages over the binning method.

Chapter 5

The Effect of the Deposition Rate and the Exclusion Principle

The deposition process is commonly modeled such that only one particle is added to the interface during each time step. The deposition rate is implicitly assumed to be merely a scale factor of little physical consequence. This assumption is justified as long the process of a particle settling on the surface takes place on a much faster timescale such that the possibility of two particles simultaneously being deposited at the same site is negligible. However, this assumption is no longer valid at sufficiently high deposition rates, and two particles could, indeed, arrive simultaneously at the same site. Here, we propose a modification to the deposition model. Namely, we introduce an exclusion principle that precludes simultaneous deposition at the same site. Physically, this restriction could be interpreted as any particle that has landed at a certain site kinetically repelling or scattering additional particles during that time step. This exclusion principle introduces a new correlation mechanism that becomes significant only when the deposition rate is sufficiently high. This modification, albeit simplistic, is motivated by experimental studies that document the importance of interactions that emerge at high deposition rates for thin films. In one study [37], the authors examined the deposition of pentacene thin films on Si/SiO_2 layers. The deposition rate (κ) was defined as the thickness changes per unit time. The change of κ for a fixed particle number was found to change the physical aspects of the system, such as the density of emerging islands, island size, and coverage. They showed that κ and density of the islands are directly proportional, and by increasing the deposition rate, the density of islands is also increased. Similarly, the particles spread over the interface when we increase the deposition rate since two particles cannot be deposited on the same column. Even though our modification is simplistic in that it does not attempt to model how the particles exclude each other, it is consistent with the island density dependence on the deposition rate. In another study [38], the authors found a minimum (3%) and a maximum value (15%) for the deposition rate for a certain material's (yttrium barium copper oxide) crystallinity. This chapter discusses the impact of deposition rate on the statistical properties of the modified ballistic and the RSOS deposition models if the exclusion principle is applied.

5.1 Ballistic Deposition Model

The simulation of the ballistic deposition model is performed using the restriction factor method discussed in the previous chapter using the following initial conditions,

- Size of the system: $N_x = 24000$
- Number of time steps: $N_t = 2500$
- Restriction factor: $RF = 14$
- Number of experiments: $N_r = 100$

5.1.1 Constant Deposition Rate

Up to now, we have chosen the deposition rate to be approximately 10% of the size of the system. For finding that if there is a relation between the size of the system and the deposition rate, we examined the statistical behavior of the system over long times. We also checked if there is a critical value for the characteristic behavior for the universality class of system changes.

In figure 5.1, the change of the skewness and kurtosis with respect to deposition rate values is shown. The red and green dashed line in the figure 5.1 shows the approximate values for 3^{rd} and 4^{th} cumulants for TW GOE distribution, respectively.

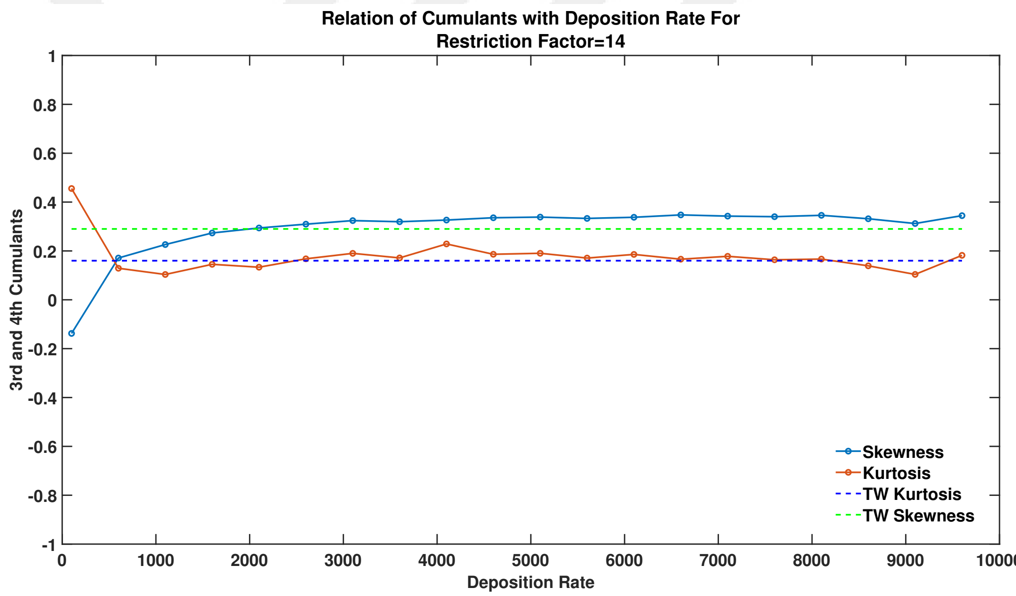

Figure 5.1: The change of 3^{rd} cumulant, skewness and 4^{th} cumulant, kurtosis with respect to the deposition rate.

In figure 5.1, for relatively small values deposition rate, $d_r = 2\%N_x$ and $d_r = 4\%N_x$, the skewness and kurtosis values are far away from the expected values for TW GOE. As we increase d_r values to the $d_r = 6\%N_x$, the skewness and kurtosis values get closer to the expected values which are $skewness = 0.29$ and $kurtosis = 3.16$. After we exceed the $d_r = 10\%N_x$, again the cumulants values diverge from the expected values. The critical values for the deposition rate are between 8% to 10% of the size of the system.

Next, we checked how the scaling exponent β changes with the deposition rate to get a better insight into the effect of the deposition rate and its relation with the size of the system. In figure 5.2 the change of the scaling exponent for surface roughness β with respect to time is plotted. For the deposition rate $d_r = 2\% N_x$, the β is far from the expected value of scaling exponent of surface roughness 1/3, as we increase the deposition rate values, the β value converges to the expected value 1/3. Compared to the TW analysis, we do not see considerable changes for the β exponent.

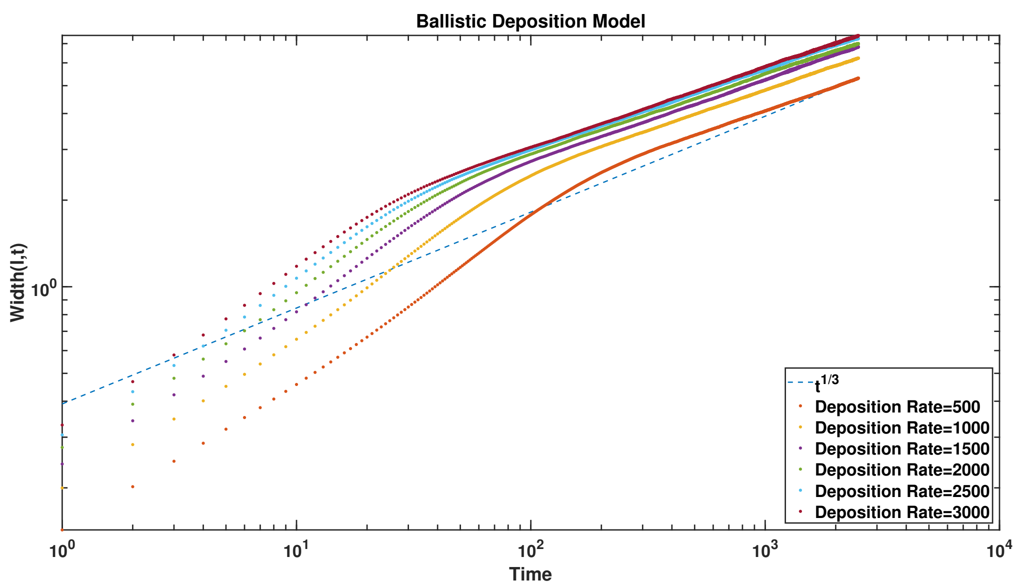

Figure 5.2: The change of width of the interface with respect to time for different deposition rate values.

In figure 5.3, the PDF of height fluctuations in logarithmic scale for different deposition rates is plotted. The histogram view also supports the previous results in figure 5.1. The best results regarding the height fluctuations are obtained for the $d_r \simeq 10\% N_x$ which have nearly 2% error with the expected results for skewness and kurtosis values of the TW GOE distribution.

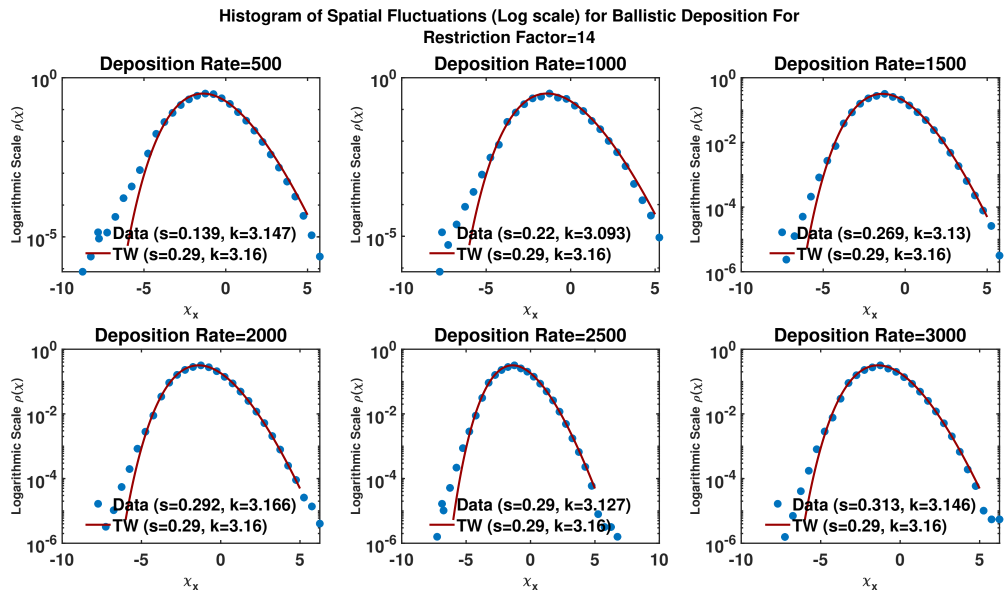

Figure 5.3: The histogram of height fluctuations for different deposition rate in logarithmic scale.

5.2 Restricted Solid-on-Solid Deposition Model

We simulated the RSOS model with the same initial values in the ballistic deposition model. The simulation's initial conditions are as follow:

- Size of the system: $N_x = 24000$
- Number of time steps: $N_t = 2500$
- Number of experiments: $N_r = 100$

In the following section, the deposition rate's effect on the RSOS model's statistical properties is discussed in detail. Due to the nature of the model itself, we expect a more stable behavior for the deposition rate change. We obtain a smoother interface because of the effect of the restriction in the RSOS model compared to the ballistic deposition model. Hence, in the RSOS model, we have more stable statistics than the ballistic deposition statistics discussed in the previous section.

5.2.1 Constant Deposition Rate

In the ballistic deposition model, the range of the deposition rate in which the statistical properties of the system agree with the KPZ universality class is too narrow, figure 5.1. For finding the effect of the deposition rate on the statistical properties of the system and its universality class, we followed the same procedure as for the ballistic deposition model.

Starting with the height fluctuations analysis. As it is known, the PDF of height fluctuations should follow the TW GOE distribution for systems in the KPZ universality class. In figure 5.4, the change of the skewness and kurtosis in distribution of height fluctuations with respect to the deposition rate is plotted. We start with the height fluctuations analysis. The PDF of height fluctuations is expected to follow the TW GOE distribution for systems in the KPZ universality class. In figure 5.4, the change of the skewness and kurtosis in the distribution of height fluctuations as a function of the deposition rate is plotted.

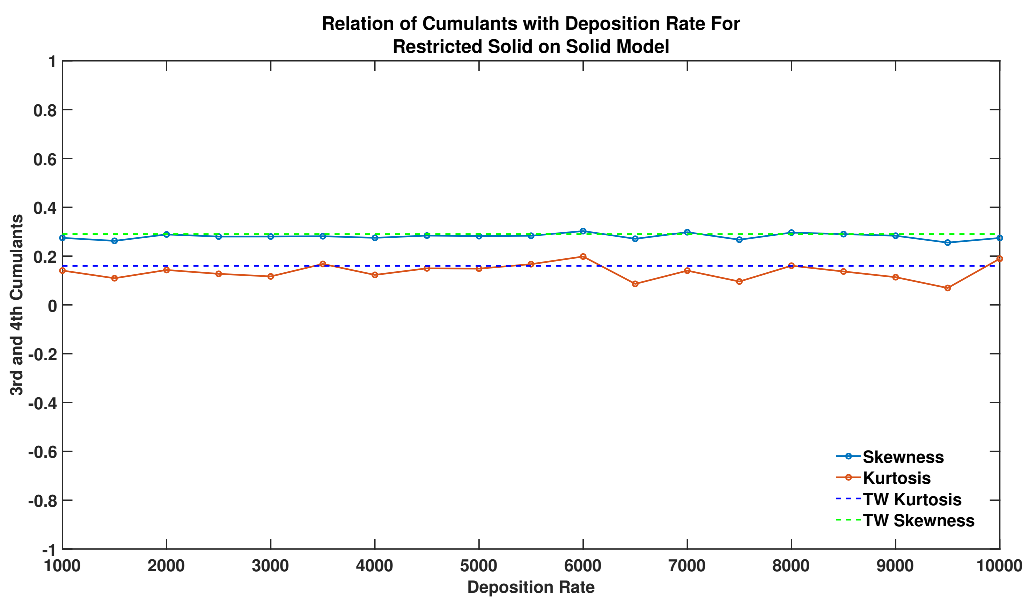

Figure 5.4: The change of 3^{rd} cumulant, skewness and 4^{th} cumulant, kurtosis with respect to the deposition rate.

From 5.4 figure, we can see that the skewness and kurtosis values are not showing high fluctuating characteristics. For small values of deposition rate,

$d_r = 1000 = 4\%N_x$ and $d_r = 1500 = 6\%N_x$, the statistics do not follow the TW GOE statistics. The results approach the TW GOE's skewness and kurtosis values at higher deposition rates. When the rate exceeds $d_r = 33\%N_x$, the statistics begin to diverge from the expected results again but remain close to skewness and kurtosis values for TW GOE. We increased the deposition rate value up to the $d_r = 75\%N_x$ to gain a better understanding (figure 5.5). The skewness value agrees with that of the TW GOE distribution, but the kurtosis value deviates substantially. From the results listed above, the critical values where the system shows statistical properties consistent with the KPZ universality class are $d_r = 8\%N_x$ and $d_r = 33\%N_x$, respectively.

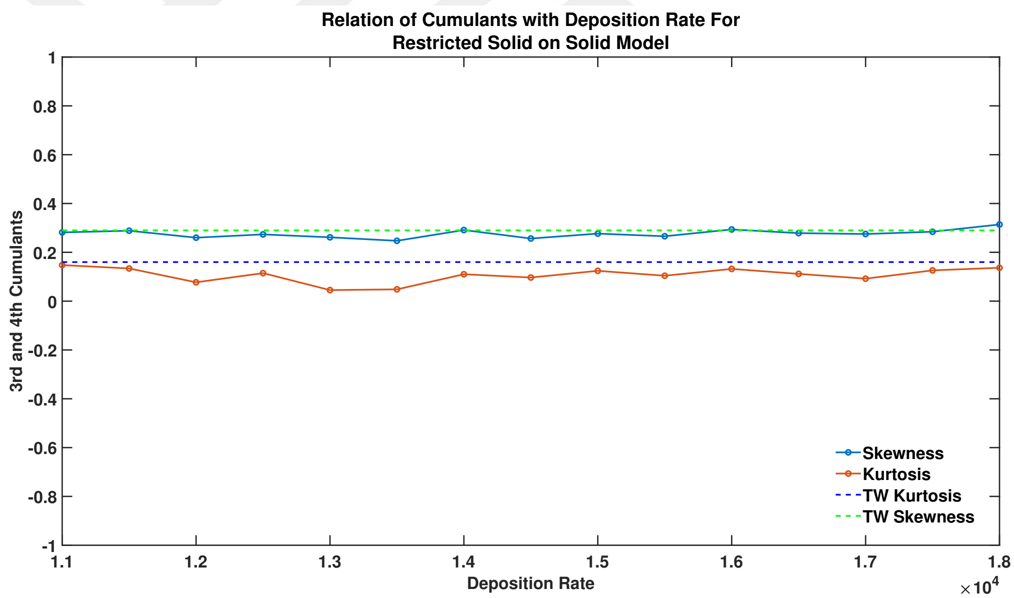

Figure 5.5: The change of 3^{rd} cumulant, skewness and 4^{th} cumulant, kurtosis with respect to the deposition rate.

Another characteristic that probes the effect of the deposition rate on the statistical properties of the system is through finding the surface roughness exponent, β. In figure 5.6, the change of width with respect to the time for six different deposition rates is shown. As it was for the ballistic deposition case, the scaling exponent β is not affected considerably by the change of the deposition rate.

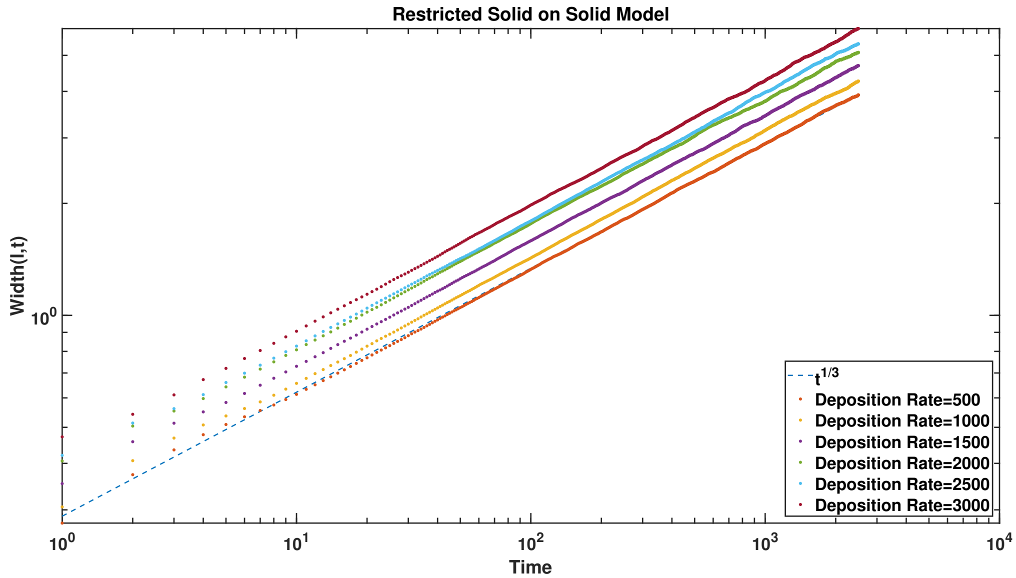

Figure 5.6: The change of width of the interface with respect to time for different deposition rate values.

While the results for the scaling exponent β are generally in good agreement with the KPZ universality class, regardless of the deposition rate, they affect the height fluctuations considerably. In figure 5.7, the histogram of height fluctuations is shown in logarithmic scale for six different deposition rates. For $d_r = 2500 \simeq 10\% N_x$, the skewness and kurtosis values are obtained to be approximately 0.29 and 3.16, respectively. As mentioned above, the best results are obtained for $d_r = \simeq 10\% N_x$, which is the same relative result as for the ballistic deposition model.

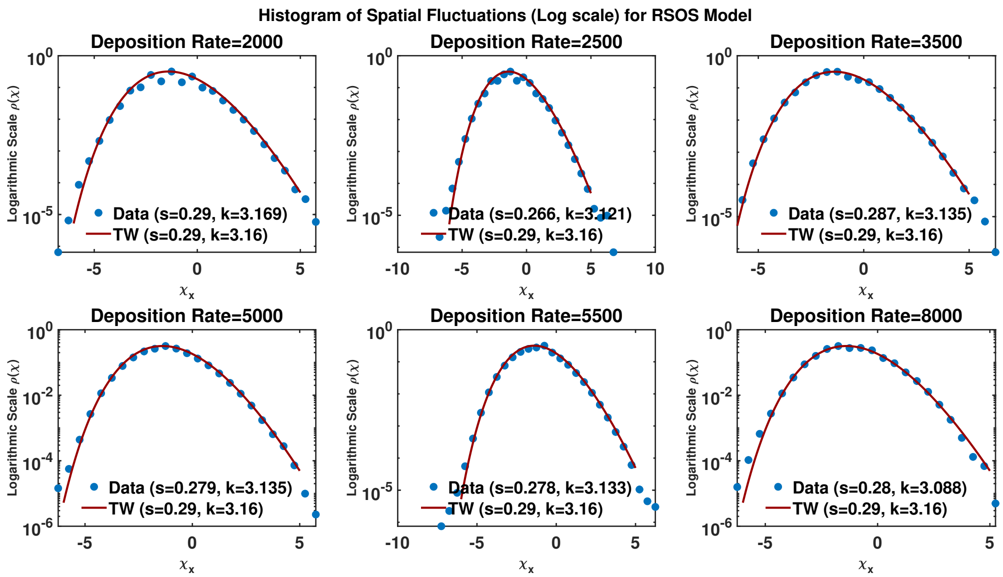

Figure 5.7: The histogram of height fluctuations for different deposition rate in logarithmic scale.

Chapter 6

Conclusion

The main goal of this thesis was to present an analysis of the statistical properties of major discrete models describing the surface growth phenomena. After describing the universality behavior of these models and their statistical properties in chapter 2, we numerically simulated five leading models in chapter 3. In chapter 3, we simulated the substrate for certain initial values in $1+1$ dimension systems for each model, except for the Eden model, which is an on-lattice model. The Eden model is described on a 2+1 dimension lattice. For each model, we calculated the width or surface roughness for obtaining the scaling exponent β and the height fluctuations distributions. For the random deposition (RD), random deposition with diffusion (RDSD), ballistic deposition (BD), Eden, and restricted solid on solid (RSOS) models, the scaling exponent, β, was calculated to be $0.50, 0.25, 0.29, 0.30$ and 0.33. The height fluctuations distribution, the skewness, and kurtosis values were calculated to be (0.06, 3.0), (0, 3.01), (0.14, 3.13), (0.23, 3.03) and (0.28, 3.17), respectively. From these results, we attributed the Gaussian, EW, KPZ universality classes to the models with skewness, kurtosis and β values as (0, 3.0, 0.5), (0, 3.0, 0.25) , and (0.29 ,3.16 ,0.33), respectively. In the BD model, our results did not fit in the KPZ universality class well due to the appearances of thin, deep wells on the interface. Such structures are not realistic but an artifact of the model. We introduced two modifications to minimize such artifacts in chapter 4. The previously known binning method was applied, but we also introduced a new method that we refer to as the restriction factor (RF) method. These modifications resulted in surface profiles that appear physically more realistic and statistical characteristics that are much closer to the expected values. Using the binning method for the scaling exponent of surface roughness, we obtained $\beta = 1/3$. For the height fluctuation distribution, we calculated the skewness to be 0.231 and kurtosis to be 3.137, which are in good agreement with the KPZ universality class. With the application of the RF method, the skewness and kurtosis values were calculated as 0.31 and 3.148, which are in good agreement with the statistics of TW GOE distribution, and hence with the KPZ universality class. In chapter 5, the effect of the change of deposition rate on our most stable, RSOS, and least stable, the ballistic deposition models, was investigated. Due to the nature of the deposition models, the system's statistical properties and universality behavior depend on the deposition rate for fixed system size. In chapter 5, we represented a detailed description of how the statistical properties of the RSOS and the ballistic deposition models change. According to the expected analytical results, we concluded that for the ballistic deposition model, the deposition rate should be around $8 - 10\% N_x$, and for the RSOS model, the deposition rate should be in the range of $(8{,}33\% N_x)$.

Finally, we wish to propose further modifications. From the experiments, [11] one can argue that the fluid flow on the system may cause the column with a bigger height to crash onto the top of its nearest neighbors. Another modification can be suggested regarding the way the particles are deposited. Usually, the deposition rate is constant in simulations. Even in laboratory experiments, this is not necessarily always the case. In natural systems, a constant rate is, at best, a rare exception. The recently introduced dynamic self-assembly method [11, 39, 40] that originally motivated this thesis involves strong feedback from the growing structure to the rest of the system, which means the deposition rate is a function of the size, shape of the surface. Consequently, the deposition rate varies dynamically. It is likely that such temporal feedback is responsible for the experimentally observed correlations in time, in addition to the well-known spatial correlations.

Bibliography

[1] R. Durrett, *Probability: theory and examples*, vol. 49. Cambridge university press, 2019.

[2] S. F. Edwards and D. Wilkinson, "The surface statistics of a granular aggregate," *Proceedings of the Royal Society of London. A. Mathematical and Physical Sciences*, vol. 381, no. 1780, pp. 17–31, 1982.

[3] F. Family, "Scaling of rough surfaces: effects of surface diffusion," *Journal of Physics A: mathematical and general*, vol. 19, no. 8, 1986.

[4] A.-L. Barabási, H. E. Stanley, *et al.*, *Fractal concepts in surface growth*. Cambridge university press, 1995.

[5] T. Halpin-Healy and Y.-C. Zhang, "Kinetic roughening phenomena, stochastic growth, directed polymers and all that. aspects of multidisciplinary statistical mechanics," *Physics reports*, vol. 254, no. 4-6, pp. 215–414, 1995.

[6] M. Kardar, G. Parisi, and Y.-C. Zhang, "Dynamic scaling of growing interfaces," *Physical Review Letters*, vol. 56, no. 9, 1986.

[7] D. Forster, D. R. Nelson, and M. J. Stephen, "Large-distance and long-time properties of a randomly stirred fluid," *Physical Review A*, vol. 16, no. 2, 1977.

[8] F. Family and T. Vicsek, "Scaling of the active zone in the eden process on percolation networks and the ballistic deposition model," *Journal of Physics A: Mathematical and General*, vol. 18, no. 2, 1985.

[9] K. A. Takeuchi and M. Sano, "Evidence for geometry-dependent universal fluctuations of the kardar-parisi-zhang interfaces in liquid-crystal turbulence," *Journal of Statistical Physics*, vol. 147, no. 5, pp. 853–890, 2012.

[10] T. Iwatsuka, Y. T. Fukai, and K. A. Takeuchi, "Direct evidence for universal statistics of stationary kardar-parisi-zhang interfaces," *Physical Review Letters*, vol. 124, no. 25, pp. 250–602, 2020.

[11] G. Makey, S. Galioglu, R. Ghaffari, E. D. Engin, G. Yıldırım, Ö. Yavuz, O. Bektaş, Ü. S. Nizam, Ö. Akbulut, Ö. Şahin, *et al.*, "Universality of dissipative self-assembly from quantum dots to human cells," *Nature Physics*, vol. 16, no. 7, pp. 795–801, 2020.

[12] G. Amir, I. Corwin, and J. Quastel, "Probability distribution of the free energy of the continuum directed random polymer in 1+ 1 dimensions," *Communications on pure and applied mathematics*, vol. 64, no. 4, pp. 466–537, 2011.

[13] T. Sasamoto and H. Spohn, "Exact height distributions for the kpz equation with narrow wedge initial condition," *Nuclear Physics B*, vol. 834, no. 3, pp. 523–542, 2010.

[14] A.-L. Barabási, H. E. Stanley, *et al.*, *Fractal concepts in surface growth.* Cambridge university press, 1995.

[15] F. Family, "Scaling of rough surfaces: effects of surface diffusion," *Journal of Physics A: mathematical and general*, vol. 19, no. 8, 1986.

[16] B. Mal, S. Ray, and J. Shamanna, "Revisiting surface diffusion in random deposition," *The European Physical Journal B*, vol. 82, no. 3, pp. 341–347, 2011.

[17] C. M. Horowitz, R. A. Monetti, and E. V. Albano, "Competitive growth model involving random deposition and random deposition with surface relaxation," *Physical Review E*, vol. 63, no. 6, pp. 066–132, 2001.

[18] M. J. Vold, "A numerical approach to the problem of sediment volume," *Journal of colloid science*, vol. 14, no. 2, pp. 168–174, 1959.

[19] M. J. Vold, "Computer simulation of floc formation in a colloidal suspension," *Journal of Colloid Science*, vol. 18, no. 7, pp. 684–695, 1963.

[20] D. N. Sutherland, "A theoretical model of floc structure," *Journal of Colloid and Interface Science*, vol. 25, no. 3, pp. 373–380, 1967.

[21] D. Bensimon, E. Domany, and A. Aharony, "Crossover of fractal dimension in diffusion-limited aggregates," *Physical Review Letters*, vol. 51, no. 15, 1983.

[22] D. Bensimon, B. Shraiman, and S. Liang, "On the ballistic model of aggregation," *Physics Letters A*, vol. 102, no. 5-6, pp. 238–240, 1984.

[23] M. Kardar, G. Parisi, and Y.-C. Zhang, "Dynamic scaling of growing interfaces," *Physical Review Letters*, vol. 56, no. 9, 1986.

[24] J. G. Amar and F. Family, "Numerical solution of a continuum equation for interface growth in 2+ 1 dimensions," *Physical Review A*, vol. 41, no. 6, 1990.

[25] A.-L. Barabási, R. Bourbonnais, M. Jensen, J. Kertész, T. Vicsek, and Y.-C. Zhang, "Multifractality of growing surfaces," *Physical Review A*, vol. 45, no. 10, 1992.

[26] T. Nagatani, "From ballistic deposition to the kardar-parisi-zhang equation through a limiting procedure," *Physical Review E*, vol. 58, no. 1, 1998.

[27] K. Banerjee, J. Shamanna, and S. Ray, "Surface morphology of a modified ballistic deposition model," *Physical Review E*, vol. 90, no. 2, pp. 022–111, 2014.

[28] T. Oliveira, S. Ferreira, and S. Alves, "Universal fluctuations in kardar-parisi-zhang growth on one-dimensional flat substrates," *Physical Review E*, vol. 85, no. 1, pp. 010–601, 2012.

[29] M. Eden *et al.*, "A two-dimensional growth process," in *Proceedings of the fourth Berkeley symposium on mathematical statistics and probability*, vol. 4, pp. 223–239, Univ of California Press Berkeley, 1961.

[30] R. Jullien and R. Botet, "Surface thickness in the eden model," *Physical review letters*, vol. 54, no. 18, 1985.

[31] S. G. Alves, T. J. Oliveira, and S. C. Ferreira, "Universal fluctuations in radial growth models belonging to the kpz universality class," *EPL (Europhysics Letters)*, vol. 96, no. 4, 2011.

[32] K. A. Takeuchi, "Statistics of circular interface fluctuations in an off-lattice eden model," *Journal of Statistical Mechanics: Theory and Experiment*, vol. 2012, no. 05, pp. P05–007, 2012.

[33] C. A. Tracy and H. Widom, "Level-spacing distributions and the airy kernel," *Communications in Mathematical Physics*, vol. 159, no. 1, pp. 151–174, 1994.

[34] A. Soshnikov, "A note on universality of the distribution of the largest eigenvalues in certain sample covariance matrices," *Journal of Statistical Physics*, vol. 108, no. 5, pp. 1033–1056, 2002.

[35] M. Prähofer and H. Spohn, "Universal distributions for growth processes in 1+ 1 dimensions and random matrices," *Physical review letters*, vol. 84, no. 21, 2000.

[36] F. Bornemann, P. L. Ferrari, and M. Prähofer, "The airy 1 process is not the limit of the largest eigenvalue in goe matrix diffusion," *Journal of Statistical Physics*, vol. 133, no. 3, pp. 405–415, 2008.

[37] S. Pratontep, M. Brinkmann, F. Nüesch, and L. Zuppiroli, "Correlated growth in ultrathin pentacene films on silicon oxide: Effect of deposition rate," *Physical Review B*, vol. 69, no. 16, pp. 165–201, 2004.

[38] X. Wu, R. Muenchausen, S. Foltyn, R. Estler, R. Dye, C. Flamme, N. Nogar, A. R. Garcia, J. Martin, and J. Tesmer, "Effect of deposition rate on properties of yba2cu3o7- δ superconducting thin films," *Applied physics letters*, vol. 56, no. 15, pp. 1481–1483, 1990.

[39] R. Ghaffari, S. Galigolu, E. D. Engin, and S. Ilday, "Dynamic self-organization of microorganisms far from equilibrium," in *APS March Meeting Abstracts*, vol. 2019, pp. H63–011, 2019.

[40] Ü. S. Nizam, G. Makey, M. Barbier, S. S. Kahraman, E. Demir, E. E. Shafigh, S. Galioglu, D. Vahabli, S. Hüsnügil, M. H. Güneş, *et al.*, "Dynamic evolution of hyperuniformity in a driven dissipative colloidal system," *Journal of Physics: Condensed Matter*, vol. 33, no. 30, pp. 304–002, 2021.

Appendix A

Code

RF Model

```
%% Run this part if you want to reproduce the whole system
    for figure 4.1, 4.2, 4.3
clc
clear
Nx=24000; % Size of the substrate in 1D system
Nt=2500;  % Number of time steps
Nr=20;    % Number of runs
dr=2500;  % deposition rate (particles per time step)
nos=5;    % Multiplication of Nr*nos gives total number of
    run
epsilonear=[1 2 3 4 5 6]; % Epsilon values for binning
Wn2store=zeros(length(epsilonear),Nt); % Storing the width
    value for each epsilon
epscount=0;
for epsilone=epsilonear
    epscount=epscount+1;
%          q_2s=0;
```

```
h_intt=zeros(Nt,Nx/epsilone); % Storing heigh values for
   each number of steps
hm=zeros(Nt,1); % mean height
w=zeros(Nt,1); % width (standard deviation of height)
h_nor=zeros(Nt,Nx/epsilone); % Normalized height values (
   Fluctuations)
h_N_nor_2=zeros(Nt,Nx/epsilone,Nr,'single'); % Storing all
    the height values for each run and each time step
w_N_2=zeros(Nt,Nr); % Empty matrix for storing the
   standard deviation data for each time step
for sss=1:nos
for r=1:Nr  % Number of runs for loop
x=1:Nx; % x index for the flat surface
h=0*x; % height according to the latest deposited
   particles per column
h_int=h; % height of the interface
h_int_e=zeros(1,Nx/epsilone);
for i=1:Nt
 xp = randperm(Nx,Nx); % the random picking of columns:
    perm then pick the first dr columns
              xc = x(xp(1:dr));

              hf=h; % temporary variable

              for m=1:length(xc)

                   x1=max([xc(m)-1 1]);% temporary variables
                   x2=xc(m);
                   x3=min([xc(m)+1 Nx]);
```

```
        if hf(x2)>=max(hf(x1),hf(x3)) % the
            deposition role (stick near next to
            highest neighbore or increase the
            height by one)
              h(xc(m))=h(xc(m))+1;
        else
             h(xc(m))=max(hf(x1),hf(x3));
        end
    end

    h_int=max([h_int;h]);  % Finding the maximum
        height which helps with constructing the
        interface
    % Finding the maximum height in the length of
        epsilon of Nx .
    % For further information on Binning method
        you can check
    % Batoul Hashemi thesis chapter 4.1
    for m=1:(Nx)/epsilone
       index=1+epsilone*(m-1);
       h_int_e(m) = max(h_int(index:index+epsilone
           -1));
    end
    h_intt(i,:)=h_int_e;

    % Calculating the fluctuations
    hm(i)=mean(h_int_e);
    w(i)=std(h_int_e);
    h_nor(i,:)=(h_intt(i,:)-hm(i))/w(i);

    % Normalizing them according to TW
    h_nor(i,:)=h_nor(i,:)*sqrt(1.607781035);
    h_nor(i,:)=h_nor(i,:) -1.2065335745820;
```

```
    % Storing the data
    h_N_nor_2(i,:,r)=h_nor(i,:);
    w_N_2(i,r)=w(i);


end %----------Nt end----------
end %----------Nr end------------
D2=h_N_nor_2(end,:,:);
DD=D2(:);
% q_2=mean(w_N_2');
% q_2s=q_2s+q_2;
ind=sss+(sss-1)*(Nx*Nr/epsilone-1);
DDstore(ind:(ind+Nx/epsilone*Nr-1))=DD;
end
% q_2av=q_2s/nos;
DD=DDstore;
% DD(DD>=5)=[];
% DD(DD<-8)=[];
s=-skewness(DD);
k=kurtosis(DD);
[N,edges] = histcounts(DD, 100,'Normalization','pdf','
    BinWidth',0.5);
N=N/max(N)*0.3175;
edges = edges(2:end) - (edges(2)-edges(1))/2;
f1=figure(1);
subplot(2,3,epscount)
semilogy(edges, N,'.','MarkerSize',30);
hold on
% xg=linspace(-6,6,100)-1.2065335745820; % domain of the
    Gaussian pdf generator
% yg=normpdf(xg,-1.2065335745820,sqrt(1.607781035)); %
    reference Gaussian PDF
% yg=yg/max(yg)*0.3175;
```

```
% Tracy_widom distribution logarithmic scale
hold on
plottwappx_log_oneD;
% plot(xg,yg,'-','color',[0.6 0.6 1],'LineWidth',2.5);
hold off
title(['\epsilon=' num2str(epsilone)],'FontSize',18)
legend(['Data (s=',num2str(round(s,3)),', k=',num2str(
   round(k,3)),')'],'TW (s=0.29, k=3.16)','FontSize',20,'
   Location','south')
legend('boxoff')
set(gca,'linewidth',1.6,'FontSize',20,'FontWeight','Bold')
xlabel('\chi_x','fontsize',16,'fontweight','bold')
ylabel('Logarithmic Scale \rho(\chi)','fontsize',15,'
   fontweight','bold')
if Nr==1
Wn2store(epsilone,:)=w_N_2';
else
Wn2store(epsilone,:)=mean(w_N_2');
end
title('Histogram of Spatial Fluctuations (Log scale) for
   RSOS Model','FontSize',20,'FontWeight','Bold')
end
%% Figure 4.1) Width vs Time needs h_int.mat file, this is
    just for the representation
Nx=120; %This is for figure 4.1, comment out if necessary.
for epsilone=1:6
h_int_e=zeros(1,Nx/epsilone);
 for m=1:Nx/epsilone
                index=1+epsilone*(m-1);
                h_int_e(m) = max(h_int(index:index+epsilone
                    -1));
 end
subplot(2,3,epsilone)
```

```
plot(h_int_e,'bO--','linewidth',1.6)
title(['Interface, \epsilon=' num2str(epsilone)],'FontSize',20)
xlabel('Nx','fontsize',30,'fontweight','bold')
ylabel('Hieght','fontsize',30,'fontweight','bold')
set(gca,'linewidth',1.6,'FontSize',20,'FontWeight','Bold')
hold on
end
%% Figure 4.2) Width vs Time needs Wn2store_binning.mat file, Nt=2500
figure(1)
Nt=2500; %Change this if you have changed the time. This is for figure 4.2.
time=1:1:Nt;
q_2=Wn2store(1,:);
loglog(time,time.^(1/3)/max(time.^(1/3))*max(q_2),'--','Linewidth',1.5)
hold on
for i=1:6
q_2=Wn2store(i,:);
loglog(time,q_2,'.','Linewidth',1.2,'Markersize',11)
%%%%%%%%%%%%%%%%%%%%%%%%%%%%%%%%%%%%%%%%%%%%%%%%%%%%
[xData, yData] = prepareCurveData( [], q_2 );
% Set up fittype and options.
ft = fittype( 'power1' );
opts = fitoptions( 'Method', 'NonlinearLeastSquares' );
opts.Display = 'Off';
opts.StartPoint = [0.47630629919212 0.350445659630466];
% Fit model to data.
[fitresult, gof] = fit( xData, yData, ft, opts );
beta=round(fitresult.b,3)
hold on
end
```

```
title('Ballistic Model','FontSize',20)
xlabel('Time','fontsize',30,'fontweight','bold')
ylabel('Width(l,t)','fontsize',30,'fontweight','bold')
set(gca,'linewidth',1.6,'FontSize',20,'FontWeight','Bold')
hold on
legend('t^{1/3}','\epsilon=1','\epsilon=2','\epsilon=3','\
    epsilon=4','\epsilon=5','\epsilon=6','Width','FontSize'
    ,20,'Location','southeast')
%% Figure 4.3) The data DD_binning_x must be in the path,
    if you run the main code,
% you do not need this part.
for epsilone=1:6
DD=importdata(['DD_binning_' num2str(epsilone) '.mat']);
s=skewness(DD);
k=kurtosis(DD);
[N,edges] = histcounts(DD, 100,'Normalization','pdf','
    BinWidth',0.5);
N=N/max(N)*0.3175;
edges = edges(2:end) - (edges(2)-edges(1))/2;
f1=figure(1);
subplot(2,3,epsilone)
semilogy(edges, N,'.','MarkerSize',30);
hold on
% xg=linspace(-6,6,100)-1.2065335745820; % domain of the
    Gaussian pdf generator
% yg=normpdf(xg,-1.2065335745820,sqrt(1.607781035)); %
    reference Gaussian PDF
% yg=yg/max(yg)*0.3175;
% Tracy_widom distribution logarithmic scale
hold on
plottwappx_log_oneD;
% plot(xg,yg,'-','color',[0.6 0.6 1],'LineWidth',2.5);
hold off
```

```
title(['\epsilon=' num2str(epsilone)],'FontSize',18)
legend(['Data (s=',num2str(round(s,3)),', k=',num2str(
    round(k,3)),')'],'TW (s=0.29, k=3.16)','FontSize',20,'
    Location','south')
legend('boxoff')
set(gca,'linewidth',1.6,'FontSize',20,'FontWeight','Bold')
xlabel('\chi_x','fontsize',16,'fontweight','bold')
ylabel('Logarithmic Scale \rho(\chi)','fontsize',15,'
    fontweight','bold')
sgtitle('Histogram of Spatial Fluctuations (Log scale) for
     Ballistic Model','FontSize',20,'FontWeight','Bold')
end
%% TW generating Function (HISTOGRAM)
function plottwappx_log_oneD

% Script to plot the approximated TW distributions
%
% see paper M.Chiani, "Distribution of the largest
    eigenvalue for real
% Wishart and Gaussian random matrices and a simple
    approximation for the
% Tracy-Widom distribution", submitted 2012, ArXiv
%
x = -6:.001:5;
[y1,z1] = tracywidom_appx(x,1);
%[y2,z2] = tracywidom_appx(x,2);
% [y4,z4] = tracywidom_appx(x,4);
% figure;
hold on

% semilogy(x,y1,x,y2,x,y4);
semilogy(x,y1,'color',[0.6, 0, 0],'LineWidth',2.5)
end
```

```
function [pdftwappx, cdftwappx] = tracywidom_appx(x, i)
%
%
% [pdftwappx, cdftwappx]=tracywidom_appx(x, i)
%
% SHIFTED GAMMA APPROXIMATION FOR THE TRACY-WIDOM LAWS, by
    M. Chiani, 2012
%
% TW ~ Gamma[k,theta]-alpha
%
% [pdf,cdf]=tracywidom_appx(x,2) gives the approximated
   pdf(x) and CDF(x) of the TW2
%
% [pdf,cdf]=tracywidom_appx(x,i) for i=1,2,4 gives TW1,
   TW2, TW4
%
% see paper M.Chiani, "Distribution of the largest
   eigenvalue for real
% Wishart and Gaussian random matrices and a simple
   approximation for the
% Tracy-Widom distribution", submitted 2012, ArXiv
%

kappx = [46.44604884387787, 79.6594870666346, 0,
   146.0206131050228];   % K, THETA, ALPHA
thetaappx = [0.18605402228279347, 0.10103655775856243, 0,
   0.05954454047933292];
alphaappx = [9.848007781128567, 9.819607173436484, 0,
   11.00161520109004];

cdftwappx = cdfgamma(x+alphaappx(i), thetaappx(i), kappx(i
   ));   % Chiani's appx: Tracy-Widom as a shifted Gamma
```

```
pdftwappx = pdfgamma(x+alphaappx(i), thetaappx(i), kappx(i
    )); % Chiani's appx: Tracy-Widom as a shifted Gamma

end

function [pdfgamma]=pdfgamma(x, ta, ka) % Utility: PDF of
    a Gamma
  if(x > 0)
      pdfgamma=1/(gamma(ka)*ta^ka) * x.^(ka - 1) .* exp(-x/
          ta);
  else
      pdfgamma=0 ;
  end
end

function[cdfgamma]=cdfgamma(x, ta, ka)  % Utility: CDF of
    a Gamma
  if(x > 0)
      cdfgamma=gammainc(x/ta,ka);
  else
      cdfgamma=0;
  end

end

%% Run this part if you want to reproduce the whole system
     for figure 4.4, 4.5, 4.6
clc
clear
Nx=24000; % Size of the substrate in 1D system
Nt=2500;  % Number of time steps
Nr=10;    % Number of runs
dr=2500;  % deposition rate (particles per time step)
```

```
nos=10;   % Multiplication of Nr*nos gives total number of
    run
Tar=[0 7 14 21 28]; % 0 means no restriction
Wn2store=zeros(length(Tar)-1,Nt);
tcount=0;
for T=Tar
   tcount=tcount+1;
h_intt=zeros(Nt,Nx); % Storing heigh values for each
   number of steps
hm=zeros(Nt,1); % mean height
w=zeros(Nt,1); % width (standard deviation of height)
h_nor=zeros(Nt,Nx); % Normalized height values (
   Fluctuations)
h_N_nor_2=zeros(Nt,Nx,Nr,'single'); % Storing all the
   height values for each run and each time step
w_N_2=zeros(Nt,Nr); % Empty matrix for storing the
   standard deviation data for each time step
DDstore=zeros(1,Nx*nos*Nr);
for sss=1:nos
for r=1:Nr  % Number of runs for loop
x=1:Nx; % x index for the flat surface
h=0*x; % height according to the latest deposited
   particles per column
h_int=h; % height of the interface

for i=1:Nt
            xp = randperm(Nx,Nx); % the random picking of
               columns: perm then pick the first dr
               columns
            xc = x(xp(1:dr));

            hf=h; % temporary variable
```

```
for m=1:length(xc)

    x1=max([xc(m)-1 1]);% temporary variables
    x2=xc(m);
    x3=min([xc(m)+1 Nx]);


    if hf(x2)>=max(hf(x1),hf(x3)) % the
       deposition role (stick near next to
       highest neighbore or increase the
       height by one)
         h(xc(m))=h(xc(m))+1;
    else
        h(xc(m))=max(hf(x1),hf(x3));
    end
end
% Finding the differenec between the heights
   and mean of all
% heights in each time step. If the height is
   more than RF the
% height is replaced with the mean height (For
     further information you can check Batuol
   Hashemi thesis 4.3)

if T>0 % For RF=0 (T=0) there is no
   restriction.
newbinning=(h_int-mean(h_int));
newbinning(newbinning<-T) = mean(h_int);
h_int=newbinning;
end
h_int=max([h_int;h]);  % Finding the maximum
   height which helps with constructing the
   interface
```

```
            h_intt(i,:)=h_int;

            % Calculating the fluctuations
            hm(i)=mean(h_int);
            w(i)=std(h_int);
            h_nor(i,:)=(h_intt(i,:)-hm(i))/w(i);

            % Normalizing them according to TW
            h_nor(i,:)=h_nor(i,:)*sqrt(1.607781035);
            h_nor(i,:)=h_nor(i,:)-1.2065335745820;

            % Storing the data
            h_N_nor_2(i,:,r)=h_nor(i,:);
            w_N_2(i,r)=w(i);


end %-----------Nt end-----------
end %-----------Nr end--------------
if T==0
    save('h_int.mat','h_int')
end
D2=h_N_nor_2(end,:,:);
DD=D2(:);
ind=sss+(sss-1)*(Nx*Nr-1);
DDstore(ind:(ind+Nx*Nr-1))=DD;
end
% q_2av=q_2s/nos;
% s=skewness(DDstore);
% k=kurtosis(DDstore);
DDD=DDstore;
DDD(DDD<-7.5)=[];
s=skewness(DDD);
```

```
k=kurtosis(DDD);
save(['DDstore_' num2str(T) '.mat'],'DDstore')
if T>0
[N,edges] = histcounts(DDD, 100,'Normalization','pdf','
    BinWidth',0.5);
N=N/max(N)*0.3175;
edges = edges(2:end) - (edges(2)-edges(1))/2;
figure(1)
subplot(2,2,tcount-1)
semilogy(edges, N,'.','MarkerSize',30);
hold on
% xg=linspace(-6,6,100)-1.2065335745820; % domain of the
    Gaussian pdf generator
% yg=normpdf(xg,-1.2065335745820,sqrt(1.607781035)); %
    reference Gaussian PDF
% yg=yg/max(yg)*0.3175;
% Tracy_widom distribution logarithmic scale
hold on
plottwappx_log_oneD;
% plot(xg,yg,'-','color',[0.6 0.6 1],'LineWidth',2.5);
hold off
title(['Restriction Factor=' num2str(T)],'FontSize',18)
legend(['Data (s=',num2str(round(s,3)),', k=',num2str(
    round(k,3)),')'],'TW (s=0.29, k=3.16)','FontSize',20,'
    Location','south')
legend('boxoff')
set(gca,'linewidth',1.6,'FontSize',20,'FontWeight','Bold')
xlabel('\chi_x','fontsize',16,'fontweight','bold')
ylabel('Logarithmic Scale \rho(\chi)','fontsize',15,'
    fontweight','bold')
if Nr==1
Wn2store(tcount,:)=w_N_2';
else
```

```
Wn2store(tcount,:)=mean(w_N_2');
end
sgtitle('Histogram of Spatial Fluctuations (Log scale) for
    Ballistic Deposition','FontSize',20,'FontWeight','Bold
   ')
end
end
%% Figure 4.4) Interface, Rf representation, needs h_int.
   mat
figure(2)
subplot(2,2,1)
plot(h_int,'bO-','linewidth',1.6)
xlim([400 450])
hold on
plot(1:length(newbinning),mean(h_int)*ones(1,length(
   newbinning)))
xlabel('Nx','fontsize',30,'fontweight','bold')
ylabel('Hieght','fontsize',30,'fontweight','bold')
title('Interface, No Restriction Factor','FontSize',20)
set(gca,'linewidth',1.6,'FontSize',20,'FontWeight','Bold')
tcount=1;
for T=[7 14 21]
    tcount=tcount+1;
            interface=h_int;
            newbinning=(h_int-mean(h_int));
            interface(newbinning<-T) = mean(h_int);
%               h_int=newbinning;

subplot(2,2,tcount)
plot(interface,'bO-','linewidth',1.6)
hold on
plot(1:length(newbinning),mean(h_int)*ones(1,length(
   newbinning)))
```

```
title(['Interface, Restriction Factor=' num2str(T)],'
   FontSize',20)
xlabel('Nx','fontsize',30,'fontweight','bold')
xlim([400 450])
ylabel('Hieght','fontsize',30,'fontweight','bold')
set(gca,'linewidth',1.6,'FontSize',20,'FontWeight','Bold')
hold on
end
%% Figure 4.5) Width vs Time, needs q_2.mat file, Nt=2500
   for figure 4.5
Nt=2500;
time=1:1:Nt;
figure(3)
q_2=Wn2store(1,:);
loglog(time,time.^(1/3)/max(time.^(1/3))*max(q_2),'--','
   Linewidth',1.5)
hold on
for i=1:4
q_2=Wn2store(i,:);
loglog(time,q_2,'.','Linewidth',1.2,'Markersize',11)
%%%%%%%%%%%%%%%%%%%%%%%%%%%%%%%%%%%%%%%%%%%%%%%%%%%%
[xData, yData] = prepareCurveData( [], q_2 );
% Set up fittype and options.
ft = fittype( 'power1' );
opts = fitoptions( 'Method', 'NonlinearLeastSquares' );
opts.Display = 'Off';
opts.StartPoint = [0.47630629919212 0.350445659630466];
% Fit model to data.
[fitresult, gof] = fit( xData, yData, ft, opts );
beta=round(fitresult.b,3)
hold on
end
title('Ballistic Deposition Model','FontSize',20)
```

```
xlabel('Time','fontsize',30,'fontweight','bold')
ylabel('Width(l,t)','fontsize',30,'fontweight','bold')
set(gca,'linewidth',1.6,'FontSize',20,'FontWeight','Bold')
hold on
legend('t^{1/3}','RF=7','RF=14','RF=21','RF=28','FontSize'
    ,20,'Location','southeast')
%% Figure 4.6)  Histogram with different deposition rates,
     needs DDstore_x.mat import files to be
% in the path. Do not run this if you reproduced the
    system.
figure(3)
tcount=0;
for T=[7 14 21 28]
     tcount=tcount+1;
DDstore=importdata(['DDstore_' num2str(T) '.mat']);
DDD=DDstore;
DDD(DDD<-7.5)=[];
s=skewness(DDD);
k=kurtosis(DDD);
[N,edges] = histcounts(DDD, 100,'Normalization','pdf','
    BinWidth',0.5);
N=N/max(N)*0.3175;
edges = edges(2:end) - (edges(2)-edges(1))/2;
subplot(2,2,tcount)
semilogy(edges, N,'.','MarkerSize',30);
hold on
% xg=linspace(-6,6,100)-1.2065335745820; % domain of the
    Gaussian pdf generator
% yg=normpdf(xg,-1.2065335745820,sqrt(1.607781035)); %
    reference Gaussian PDF
% yg=yg/max(yg)*0.3175;
% Tracy_widom distribution logarithmic scale
hold on
```

```
plottwappx_log_oneD;
% plot(xg,yg,'-','color',[0.6 0.6 1],'LineWidth',2.5);
hold off
title(['Restriction Factor=' num2str(T)],'FontSize',18)
legend(['Data (s=',num2str(round(s,3)),', k=',num2str(
   round(k,3)),')'],'TW (s=0.29, k=3.16)','FontSize',20,'
   Location','south')
legend('boxoff')
set(gca,'linewidth',1.6,'FontSize',20,'FontWeight','Bold')
xlabel('\chi_x','fontsize',16,'fontweight','bold')
ylabel('Logarithmic Scale \rho(\chi)','fontsize',15,'
   fontweight','bold')
sgtitle('Histogram of Spatial Fluctuations (Log scale) for
    Ballistic Deposition','FontSize',20,'FontWeight','Bold
   ')
end
%% TW generating Function (HISTOGRAM)
function plottwappx_log_oneD

% Script to plot the approximated TW distributions
%
% see paper M.Chiani, "Distribution of the largest
   eigenvalue for real
% Wishart and Gaussian random matrices and a simple
   approximation for the
% Tracy-Widom distribution", submitted 2012, ArXiv
%
x = -6:.001:5;
[y1,z1] = tracywidom_appx(x,1);
%[y2,z2] = tracywidom_appx(x,2);
% [y4,z4] = tracywidom_appx(x,4);
% figure;
hold on
```

```
% semilogy(x,y1,x,y2,x,y4);
semilogy(x,y1,'color',[0.6, 0, 0],'LineWidth',2.5)
end

function [pdftwappx, cdftwappx] = tracywidom_appx(x, i)
%
%
% [pdftwappx, cdftwappx]=tracywidom_appx(x, i)
%
% SHIFTED GAMMA APPROXIMATION FOR THE TRACY-WIDOM LAWS, by
    M. Chiani, 2012
%
% TW ~ Gamma[k,theta]-alpha
%
% [pdf,cdf]=tracywidom_appx(x,2) gives the approximated
    pdf(x) and CDF(x) of the TW2
%
% [pdf,cdf]=tracywidom_appx(x,i) for i=1,2,4 gives TW1,
    TW2, TW4
%
% see paper M.Chiani, "Distribution of the largest
    eigenvalue for real
% Wishart and Gaussian random matrices and a simple
    approximation for the
% Tracy-Widom distribution", submitted 2012, ArXiv
%

kappx = [46.44604884387787, 79.6594870666346, 0,
    146.0206131050228];   % K, THETA, ALPHA
thetaappx = [0.186054022228279347, 0.101036557758562243, 0,
    0.0595445404793 3292];
```

```
alphaappx = [9.848007781128567, 9.819607173436484, 0,
    11.00161520109004];

cdftwappx = cdfgamma(x+alphaappx(i), thetaappx(i), kappx(i
    ));    % Chiani's appx: Tracy—Widom as a shifted Gamma

pdftwappx = pdfgamma(x+alphaappx(i), thetaappx(i), kappx(i
    ));    % Chiani's appx: Tracy—Widom as a shifted Gamma

end

function  [pdfgamma]=pdfgamma(x, ta, ka) % Utility: PDF of
    a Gamma
  if(x > 0)
      pdfgamma=1/(gamma(ka)*ta^ka) * x.^(ka - 1) .* exp(-x/
          ta);
  else
      pdfgamma=0  ;
  end
end

function [cdfgamma]=cdfgamma(x, ta, ka)  % Utility: CDF of
    a Gamma
  if(x > 0)
      cdfgamma=gammainc(x/ta,ka);
  else
      cdfgamma=0;
  end

end

%% Run this part if you want to reproduce the whole system
    for figure 4.8
clc
```

```
clear
close all
Nx=24000; % Size of the substrate in 1D system
Nt=2500;  % Number of time steps
dr=2500;  % deposition rate (particles per time step)
Nr=20;    % Number of runs
nos=10;   % Multiplication of Nr*nos gives total number of
    run
T=14;     % Restritcion factor
h_intt=zeros(Nt,Nx); % Storing heigh values for each
   number of steps
hm=zeros(Nt,1); % mean height
w=zeros(Nt,1); % width (standard deviation of height)
h_nor=zeros(Nt,Nx); % Normalized height values (
   Fluctuations)
h_N_nor_2=zeros(Nt,Nx,Nr,'single'); % Storing all the
   height values for each run and each time step
w_N_2=zeros(Nt,Nr); % Empty matrix for storing the
   standard deviation data for each time step
DDstore=zeros(1,Nx*nos*Nr);
for sss=1:nos
for r=1:Nr  % Number of runs for loop
x=1:Nx; % x index for the flat surface
h=0*x; % height according to the latest deposited
   particles per column
h_int=h; % height of the interface

for i=1:Nt
            xp = randperm(Nx,Nx); % the random picking of
               columns: perm then pick the first dr
               columns
            xc = x(xp(1:dr));
```

```
hf=h; % temporary variable

for m=1:length(xc)

    x1=max([xc(m)-1 1]);% temporary variables
    x2=xc(m);
    x3=min([xc(m)+1 Nx]);


    if hf(x2)>=max(hf(x1),hf(x3)) % the
       deposition role (stick near next to
       highest neighbore or increase the
       height by one)
         h(xc(m))=h(xc(m))+1;
    else
        h(xc(m))=max(hf(x1),hf(x3));
    end
end
 % Finding the differenec between the heights
     and mean of all
% heights in each time step. If the height is
    more than RF the
% height is replaced with the mean height (For
     further information you can check Batuol
    Hashemi thesis 4.3)
newbinning=(h_int-mean(h_int));
newbinning(newbinning<-T) = mean(h_int);
h_int=newbinning;

h_int=max([h_int;h]);  % Finding the maximum
    height which helps with constructing the
    interface
h_intt(i,:)=h_int;
```

```
% Calculating the fluctuations
hm(i)=mean(h_int);
w(i)=std(h_int);
h_nor(i,:)=(h_intt(i,:)-hm(i))/w(i);

% Normalizing them according to TW
h_nor(i,:)=h_nor(i,:)*sqrt(1.607781035);
h_nor(i,:)=h_nor(i,:)-1.2065335745820;
% Storing the data
h_N_nor_2(i,:,r)=h_nor(i,:);
w_N_2(i,r)=w(i);
end %----------Nt end------------
end %----------Nr end---------------
D2=h_N_nor_2(end,:,:);
DD=D2(:);
ind=sss+(sss-1)*(Nx*Nr-1);
DDstore(ind:(ind+Nx*Nr-1))=DD;
end
%% Figure 4.8) Histogram of Ballisic with rf method rf=14,
    needs DDstore.mat
figure(1)

s=skewness(DDstore);
k=kurtosis(DDstore);
[N,edges] = histcounts(DDstore, 100,'Normalization','pdf',
   'BinWidth',0.5);
N=N/max(N)*0.3175;
edges = edges(2:end) - (edges(2)-edges(1))/2;
semilogy(edges, N,'.','MarkerSize',30);
hold on
% xg=linspace(-6,6,100)-1.2065335745820; % domain of the
   Gaussian pdf generator
```

```
% yg=normpdf(xg,-1.2065335745820,sqrt(1.607781035)); %
    reference Gaussian PDF
% yg=yg/max(yg)*0.3175;
% Tracy_widom distribution logarithmic scale
hold on
plottwappx_log_oneD;
% plot(xg,yg,'-','color',[0.6 0.6 1],'LineWidth',2.5);
hold off
legend(['Data (s=',num2str(round(s,3)),', k=',num2str(
    round(k,3)),')'],'TW (s=0.29, k=3.16)','FontSize',20,'
    Location','south')
legend('boxoff')
set(gca,'linewidth',1.6,'FontSize',20,'FontWeight','Bold')
xlabel('\chi_x','fontsize',16,'fontweight','bold')
ylabel('Logarithmic Scale \rho(\chi)','fontsize',15,'
    fontweight','bold')
title({'Histogram of Spatial Fluctuations (Log scale) for
    Ballistic Deposition For', 'Restriction Factor=14'},'
    FontSize',20,'FontWeight','Bold')
%% TW generating Function (HISTOGRAM)
function plottwappx_log_oneD

% Script to plot the approximated TW distributions
%
% see paper M.Chiani, "Distribution of the largest
    eigenvalue for real
% Wishart and Gaussian random matrices and a simple
    approximation for the
% Tracy-Widom distribution", submitted 2012, ArXiv
%
x = -6:.001:5;
[y1,z1] = tracywidom_appx(x,1);
%[y2,z2] = tracywidom_appx(x,2);
```

```
% [y4,z4] = tracywidom_appx(x,4);
% figure;
hold on

% semilogy(x,y1,x,y2,x,y4);
semilogy(x,y1,'color',[0.6, 0, 0],'LineWidth',2.5)
end

function [pdftwappx, cdftwappx] = tracywidom_appx(x, i)
%
%
% [pdftwappx, cdftwappx]=tracywidom_appx(x, i)
%
% SHIFTED GAMMA APPROXIMATION FOR THE TRACY-WIDOM LAWS, by
    M. Chiani, 2012
%
% TW ~ Gamma[k,theta]-alpha
%
% [pdf,cdf]=tracywidom_appx(x,2) gives the approximated
    pdf(x) and CDF(x) of the TW2
%
% [pdf,cdf]=tracywidom_appx(x,i) for i=1,2,4 gives TW1,
    TW2, TW4
%
% see paper M.Chiani, "Distribution of the largest
    eigenvalue for real
% Wishart and Gaussian random matrices and a simple
    approximation for the
% Tracy-Widom distribution", submitted 2012, ArXiv
%

kappx = [46.44604884387787, 79.6594870666346, 0,
    146.0206131050228];   % K, THETA, ALPHA
```

```
thetaappx = [0.18605402228279347, 0.10103655775856243, 0,
    0.05954454047933292];
alphaappx = [9.848007781128567, 9.819607173436484, 0,
    11.00161520109004];

cdftwappx = cdfgamma(x+alphaappx(i), thetaappx(i), kappx(i
    ));   % Chiani's appx: Tracy—Widom as a shifted Gamma

pdftwappx = pdfgamma(x+alphaappx(i), thetaappx(i), kappx(i
    ));   % Chiani's appx: Tracy—Widom as a shifted Gamma

end

function [pdfgamma]=pdfgamma(x, ta, ka) % Utility: PDF of
    a Gamma
 if(x > 0)
      pdfgamma=1/(gamma(ka)*ta^ka) * x.^(ka - 1) .* exp(-x/
          ta);
 else
      pdfgamma=0 ;
 end
end

function[cdfgamma]=cdfgamma(x, ta, ka)  % Utility: CDF of
    a Gamma
 if(x > 0)
      cdfgamma=gammainc(x/ta,ka);
 else
      cdfgamma=0;
 end

end
```

```
%% Run this part if you want to reproduce the whole system for figure 5.1
clc
clear
Nx=24000; % Size of the substrate in 1D system
Nt=2500;  % Number of time steps
Nr=20;    % Number of runs
nos=5;    % Number of saves (Total number of runs = Nr*nos)
T=14;     % Chosen RF value

drar=100:500:10000; % deposition rate (particles per time step)
sstore=zeros(1,length(drar)); % Storing the skewness value for each deposition rate value
kstore=zeros(1,length(drar)); % Storing the kurtosis value for each deposition rate value
dpct=0;
for dr=drar
    dpct=dpct+1;
clearvars -except Nx Nt Nr nos dr T dpct Wn2store epsilone drar sstore kstore
h_intt=zeros(Nt,Nx); % Storing heigh values for each number of steps
hm=zeros(Nt,1); % mean height
w=zeros(Nt,1); % width (standard deviation of height)
h_nor=zeros(Nt,Nx); % Normalized height values (Fluctuations)
h_N_nor_2=zeros(Nt,Nx,Nr,'single');
w_N_2=zeros(Nt,Nr); % Empty matrix for storing the standard deviation data for each time step
DDstore=zeros(1,Nx*nos*Nr);
for sss=1:nos
```

```
for r=1:Nr
x=1:Nx; % x index for the flat surface
h=0*x; % height according to the latest deposited
   particles per column
h_int=h; % height of the interface

for i=1:Nt
            xp = randperm(Nx,Nx); % the random picking of
               columns: perm then pick the first dr
               columns
            xc = x(xp(1:dr));

            hf=h; % temporary variable

            for m=1:length(xc)

                x1=max([xc(m)-1 1]);% temporary variables
                x2=xc(m);
                x3=min([xc(m)+1 Nx]);


                if hf(x2)>=max(hf(x1),hf(x3)) % the
                   deposition role (stick near next to
                   highest neighbore or increase the
                   height by one)
                     h(xc(m))=h(xc(m))+1;
                else
                    h(xc(m))=max(hf(x1),hf(x3));
                end
            end

            % Finding the height difference of each point
               with respect to
```

```
            % the mean height at each time step. Replacing
                it when it is
            % hole with depth greater than the chosen RF
               value for more
            % information read chapter 4.2 and chapter 5
               of Batoul Hashemi
            % thesis
            newbinning=(h_int-mean(h_int));
            newbinning(newbinning<-T) = mean(h_int);


            h_int=newbinning;
            h_int=max([h_int;h]);

            h_intt(i,:)=h_int;

            % Calculating the fluctuations
            hm(i)=mean(h_int);
            w(i)=std(h_int);
            h_nor(i,:)=(h_intt(i,:)-hm(i))/w(i);
            % Normalizing the fluctuatuions value with
               respect to the TW
            h_nor(i,:)=h_nor(i,:)*sqrt(1.607781035);
            h_nor(i,:)=h_nor(i,:) -1.2065335745820;

            h_N_nor_2(i,:,r)=h_nor(i,:);
end %-----------Nt end-----------
end %-----------Nr end-------------
D2=h_N_nor_2(end,:,:);
DD=D2(:);
ind=sss+(sss-1)*(Nx*Nr-1);
DDstore(ind:(ind+Nx*Nr-1))=DD;
end
```

```
s=skewness(DDstore);
k=kurtosis(DDstore);
sstore(dpct)=s;
kstore(dpct)=k;
end
%% Figure 5.1) Skewness-Kurtosis analysis for RF=14, needs sstore.mat and kstore.mat
drar=100:500:10000; %Comment out this if you reproduced different array
f=figure(1);
plot(drar,sstore,'o-','linewidth',2)
hold on
plot(drar,3-kstore,'o-','linewidth',2)
plot(drar,0.16*ones(1,length(drar)),'b--','linewidth',2)
plot(drar,0.29*ones(1,length(drar)),'g--','linewidth',2)
title({'Relation of Cumulants with Deposition Rate For',['Restriction Factor=' num2str(T)]},'FontSize',18)
legend('Skewness','Kurtosis','TW Kurtosis','TW Skewness','FontSize',20,'Location','Best')
legend('boxoff')
ylim([-1 1])
set(gca,'linewidth',1.6,'FontSize',20,'FontWeight','Bold')
xlabel('Deposition Rate','fontsize',20,'fontweight','bold')
ylabel('3rd and 4th Cumulants','fontsize',20,'fontweight','bold')
save(f,'skew, kurt vs deposition rate ballistic rf.fig')
%%
function plottwappx_log_oneD

% Script to plot the approximated TW distributions
%
```

```
% see paper M.Chiani, "Distribution of the largest
    eigenvalue for real
% Wishart and Gaussian random matrices and a simple
    approximation for the
% Tracy-Widom distribution", submitted 2012, ArXiv
%
x = -6:.001:5;
[y1,z1] = tracywidom_appx(x,1);
%[y2,z2] = tracywidom_appx(x,2);
% [y4,z4] = tracywidom_appx(x,4);
% figure;
hold on

% semilogy(x,y1,x,y2,x,y4);
semilogy(x,y1,'color',[0.6, 0, 0],'LineWidth',2.5)
end

function [pdftwappx, cdftwappx] = tracywidom_appx(x, i)
%
%
% [pdftwappx, cdftwappx]=tracywidom_appx(x, i)
%
% SHIFTED GAMMA APPROXIMATION FOR THE TRACY-WIDOM LAWS, by
     M. Chiani, 2012
%
% TW ~ Gamma[k,theta]-alpha
%
% [pdf,cdf]=tracywidom_appx(x,2) gives the approximated
    pdf(x) and CDF(x) of the TW2
%
% [pdf,cdf]=tracywidom_appx(x,i) for i=1,2,4 gives TW1,
    TW2, TW4
%
```

```
% see paper M.Chiani, "Distribution of the largest eigenvalue for real
% Wishart and Gaussian random matrices and a simple approximation for the
% Tracy-Widom distribution", submitted 2012, ArXiv
%

kappx = [46.44604884387787, 79.6594870666346, 0, 146.0206131050228];   % K, THETA, ALPHA
thetaappx = [0.18605402228279347, 0.10103655775856243, 0, 0.05954454047933292];
alphaappx = [9.848007781128567, 9.819607173436484, 0, 11.00161520109004];

cdftwappx = cdfgamma(x+alphaappx(i), thetaappx(i), kappx(i));   % Chiani's appx: Tracy-Widom as a shifted Gamma

pdftwappx = pdfgamma(x+alphaappx(i), thetaappx(i), kappx(i));   % Chiani's appx: Tracy-Widom as a shifted Gamma

end

function [pdfgamma]=pdfgamma(x, ta, ka) % Utility: PDF of a Gamma
 if(x > 0)
     pdfgamma=1/(gamma(ka)*ta^ka) * x.^(ka - 1) .* exp(-x/ta);
 else
     pdfgamma=0 ;
 end
end
```

```
function [cdfgamma]=cdfgamma(x, ta, ka)  % Utility: CDF of
    a Gamma
  if(x > 0)
        cdfgamma=gammainc(x/ta,ka);
  else
        cdfgamma=0;
  end
end

%% Run this part if you want to reproduce the whole system
     for figure 5.2, 5.3
clc
clear
Nx=24000; % Size of the substrate in 1D system
Nt=2500;  % Number of time steps
Nr=20;    % Number of runs
nos=5;    % Number of saves (Total number of runs = Nr*nos
    )
T=14;     % Setting restriction factor to 14
dpct=0;
Wn2store=zeros(6,Nt);
for dr=[500 1000 1500 2000 2500 3000]  % deposition rate (
    particles per time step)
     dpct=dpct+1;
clearvars -except Nx Nt Nr nos dr T dpct Wn2store
h_intt=zeros(Nt,Nx);  % Storing heigh values for each
    number of steps
hm=zeros(Nt,1); % mean height
w=zeros(Nt,1); % width (standard deviation of height)
h_nor=zeros(Nt,Nx); % Normalized height values (
    Fluctuations)
h_N_nor_2=zeros(Nt,Nx,Nr,'single');
w_N_2=zeros(Nt,Nr);  % Empty matrix for storing the
    standard deviation data for each time step
```

```
DDstore=zeros(1,Nx*nos*Nr);
for sss=1:nos
for r=1:Nr % Number of runs for loop
x=1:Nx; % x index for the flat surface
h=0*x; % height according to the latest deposited particles per column
h_int=h; % height of the interface

for i=1:Nt
            xp = randperm(Nx,Nx); % the random picking of columns: perm then pick the first dr columns
            xc = x(xp(1:dr));

            hf=h; % temporary variable

            for m=1:length(xc)

                x1=max([xc(m)-1 1]);% temporary variables
                x2=xc(m);
                x3=min([xc(m)+1 Nx]);


                if hf(x2)>=max(hf(x1),hf(x3)) % the deposition role (stick near next to highest neighbore or increase the height by one)
                    h(xc(m))=h(xc(m))+1;
                else
                    h(xc(m))=max(hf(x1),hf(x3));
                end
            end
```

```
            % Finding the height difference of each point
                with respect to
            % the mean height at each time step. Replacing
                 it when it is
            % hole with depth greater than the chosen RF
                value for more
            % information read chapter 4.2 and chapter 5
                of Batoul Hashemi
            % thesis
            newbinning=(h_int-mean(h_int));
            newbinning(newbinning<-T) = mean(h_int);


            h_int=newbinning;
            h_int=max([h_int;h]);

            h_intt(i,:)=h_int;

            % Calculating the fluctuations
            hm(i)=mean(h_int);
            w(i)=std(h_int);
            h_nor(i,:)=(h_intt(i,:)-hm(i))/w(i);

            % Normalizing them according to TW
            h_nor(i,:)=h_nor(i,:)*sqrt(1.607781035);
            h_nor(i,:)=h_nor(i,:) -1.2065335745820;

            h_N_nor_2(i,:,r)=h_nor(i,:);
            w_N_2(i,r)=w(i);
end %------------Nt end------------
end %------------Nr end--------------
D2=h_N_nor_2(end,:,:);
DD=D2(:);
```

```
ind=sss+(sss-1)*(Nx*Nr-1);
DDstore(ind:(ind+Nx*Nr-1))=DD;
end
% q_2av=q_2s/nos;
s=skewness(DDstore);
k=kurtosis(DDstore);
[N,edges] = histcounts(DDstore, 100,'Normalization','pdf',
    'BinWidth',0.5);
N=N/max(N)*0.3175;
edges = edges(2:end) - (edges(2)-edges(1))/2;
figure(1)
subplot(2,3,dpct)
semilogy(edges, N,'.','MarkerSize',30);
hold on
% xg=linspace(-6,6,100)-1.2065335745820; % domain of the
    Gaussian pdf generator
% yg=normpdf(xg,-1.2065335745820,sqrt(1.607781035)); %
    reference Gaussian PDF
% yg=yg/max(yg)*0.3175;
% Tracy_widom distribution logarithmic scale
hold on
plottwappx_log_oneD;
% plot(xg,yg,'-','color',[0.6 0.6 1],'LineWidth',2.5);
hold off
title(['Deposition Rate=' num2str(dr)],'FontSize',18)
legend(['Data (s=',num2str(round(s,3)),', k=',num2str(
    round(k,3)),')'],'TW (s=0.29, k=3.16)','FontSize',20,'
    Location','south')
legend('boxoff')
set(gca,'linewidth',1.6,'FontSize',20,'FontWeight','Bold')
xlabel('\chi_x','fontsize',16,'fontweight','bold')
ylabel('Logarithmic Scale \rho(\chi)','fontsize',15,'
    fontweight','bold')
```

```
if Nr==1
Wn2store(dpct,:)=w_N_2';
else
Wn2store(dpct,:)=mean(w_N_2');
end
sgtitle({'Histogram of Spatial Fluctuations (Log scale)
   for Ballistic Deposition For', 'Restriction Factor=14'
   },'FontSize',20,'FontWeight','Bold')
end
%% Figure 5.2) Width vs Time, needs Wn2store_rf.mat file,
    Nt=2500 for figure 5.2
Nt=2500;
time=1:1:Nt;
figure(2)
q_2=Wn2store(1,:);
loglog(time,time.^(1/3)/max(time.^(1/3))*max(q_2),'--','
   Linewidth',1.5)
hold on
% for i=1
for i=1:6
q_2=Wn2store(i,:);
loglog(time,q_2,'.','Linewidth',1.2,'Markersize',11)
%%%%%%%%%%%%%%%%%%%%%%%%%%%%%%%%%%%%%%%%%%%%%%%%%%%%%%%%
[xData, yData] = prepareCurveData( [], q_2 );
% Set up fittype and options.
ft = fittype( 'power1' );
opts = fitoptions( 'Method', 'NonlinearLeastSquares' );
opts.Display = 'Off';
opts.StartPoint = [0.47630629919212 0.350445659630466];
% Fit model to data.
[fitresult, gof] = fit( xData, yData, ft, opts );
beta=round(fitresult.b,3)
hold on
```

```
end
title('Ballistic Deposition Model','FontSize',20)
xlabel('Time','fontsize',30,'fontweight','bold')
ylabel('Width(l,t)','fontsize',30,'fontweight','bold')
set(gca,'linewidth',1.6,'FontSize',20,'FontWeight','Bold')
hold on
legend('t^{1/3}','Deposition Rate=500','Deposition Rate
    =1000','Deposition Rate=1500','Deposition Rate=2000','
    Deposition Rate=2500','Deposition Rate=3000','FontSize'
    ,20,'Location','southeast')
%% Figure 5.3) Histogram with different deposition rates,
     needs DDstore_rf_x.mat import files to be
% in the path. Do not run this if you reproduce the system
    .
figure(3)
dpct=0;
for dr=[500 1000 1500 2000 2500 3000]
     dpct=dpct+1;
DDstore=importdata(['DDstore_rf_' num2str(dr) '.mat']);
s=skewness(DDstore);
k=kurtosis(DDstore);
[N,edges] = histcounts(DDstore, 100,'Normalization','pdf',
    'BinWidth',0.5);
N=N/max(N)*0.3175;
edges = edges(2:end) - (edges(2)-edges(1))/2;
subplot(2,3,dpct)
semilogy(edges, N,'.','MarkerSize',30);
hold on
% xg=linspace(-6,6,100)-1.2065335745820; % domain of the
    Gaussian pdf generator
% yg=normpdf(xg,-1.2065335745820,sqrt(1.607781035)); %
    reference Gaussian PDF
% yg=yg/max(yg)*0.3175;
```

```
% Tracy_widom distribution logarithmic scale
hold on
plottwappx_log_oneD;
% plot(xg,yg,'-','color',[0.6 0.6 1],'LineWidth',2.5);
hold off
title(['Deposition Rate=' num2str(dr)],'FontSize',18)
legend(['Data (s=',num2str(round(s,3)),', k=',num2str(
    round(k,3)),')'],'TW (s=0.29, k=3.16)','FontSize',20,'
    Location','south')
legend('boxoff')
set(gca,'linewidth',1.6,'FontSize',20,'FontWeight','Bold')
xlabel('\chi_x','fontsize',16,'fontweight','bold')
ylabel('Logarithmic Scale \rho(\chi)','fontsize',15,'
    fontweight','bold')
sgtitle({'Histogram of Spatial Fluctuations (Log scale)
    for Ballistic Deposition For', 'Restriction Factor=14'
    },'FontSize',20,'FontWeight','Bold')
end
%%
function plottwappx_log_oneD

% Script to plot the approximated TW distributions
%
% see paper M. Chiani, "Distribution of the largest
    eigenvalue for real
% Wishart and Gaussian random matrices and a simple
    approximation for the
% Tracy-Widom distribution", submitted 2012, ArXiv
%
x = -6:.001:5;
[y1,z1] = tracywidom_appx(x,1);
%[y2,z2] = tracywidom_appx(x,2);
% [y4,z4] = tracywidom_appx(x,4);
```

```
% figure;
hold on

% semilogy(x,y1,x,y2,x,y4);
semilogy(x,y1,'color',[0.6, 0, 0],'LineWidth',2.5)
end

function [pdftwappx, cdftwappx] = tracywidom_appx(x, i)
%
%
% [pdftwappx, cdftwappx]=tracywidom_appx(x, i)
%
% SHIFTED GAMMA APPROXIMATION FOR THE TRACY-WIDOM LAWS, by
    M. Chiani, 2012
%
% TW ~ Gamma[k,theta]-alpha
%
% [pdf,cdf]=tracywidom_appx(x,2) gives the approximated
    pdf(x) and CDF(x) of the TW2
%
% [pdf,cdf]=tracywidom_appx(x,i) for i=1,2,4 gives TW1,
    TW2, TW4
%
% see paper M.Chiani, "Distribution of the largest
    eigenvalue for real
% Wishart and Gaussian random matrices and a simple
    approximation for the
% Tracy-Widom distribution", submitted 2012, ArXiv
%

kappx = [46.44604884387787, 79.6594870666346, 0,
    146.0206131050228];    % K, THETA, ALPHA
```

```
thetaappx = [0.18605402228279347, 0.10103655775856243, 0,
    0.05954454047933292];
alphaappx = [9.848007781128567, 9.819607173436484, 0,
    11.00161520109004];

cdftwappx = cdfgamma(x+alphaappx(i), thetaappx(i), kappx(i
    )); % Chiani's appx: Tracy-Widom as a shifted Gamma

pdftwappx = pdfgamma(x+alphaappx(i), thetaappx(i), kappx(i
    )); % Chiani's appx: Tracy-Widom as a shifted Gamma

end

function [pdfgamma]=pdfgamma(x, ta, ka) % Utility: PDF of
    a Gamma
 if(x > 0)
      pdfgamma=1/(gamma(ka)*ta^ka) * x.^(ka - 1) .* exp(-x/
          ta);
 else
      pdfgamma=0 ;
 end
end

function[cdfgamma]=cdfgamma(x, ta, ka)  % Utility: CDF of
    a Gamma
 if(x > 0)
      cdfgamma=gammainc(x/ta,ka);
 else
      cdfgamma=0;
 end

end
```